JLAB-TN-05-049

# FINITE ELEMENT ANALYSIS OF FEL OC MIRROR

Katherine M. Wilson
2 May 2005

The FEL output coupler (OC) mirror is a slightly concave sapphire mirror, cryogenically cooled to combat the heat load from the laser which impacts upon it. In order for the mirror to function properly, it must not expand in the axial direction by more than 35 nm due to heating. An analysis was performed to determine the thermal profile of the mirror and the resulting deflections.

## I. Heat Loads

For 1 kW heat output, there are four heat loads on the mirror:

a. Fundamental: 2.2 W applied in a Gaussian profile over a 6 mm radius on the surface of the mirror
b. 2nd harmonic: 10 W applied in a Gaussian profile over a 3.2 mm radius on the surface of the mirror
c. 3rd harmonic: 1 W applied in a Gaussian profile over a 2.14 mm radius on the surface of the mirror
d. Bulk heat load: 19.1 W on a 0.375 inch thick mirror applied in a Gaussian profile over a 6 mm radius through the bulk material

These heat loads are superimposed. Loads (b) and (c) are unlikely to change, so a margin of 50% is applied only to loads (a) and (d): the fundamental surface load becomes 3.3 W and the bulk heat load becomes 28.65 W, for a total of ~ 43 W.

### A. Bulk Heat Load

The bulk heat load is applied to a cylinder with radius 0.012 m cut along the axis of the mirror. The total heat load applied is 28.65 W. The heat load does not vary with thickness, though, obviously, it varies with radius.

The Gaussian profile is $P = \dfrac{2 * Pav}{\pi * \omega^2 * \exp(\frac{2r^2}{\omega^2})}$ where P is the power density.

Where $\omega = 0.006$ m and $\omega^2 = 0.000036$ m$^2$
Pav = 28.65 W

$$\rightarrow P = \frac{2 * 28.65}{\pi * 0.000036 * \exp(\frac{2r^2}{0.000036})}$$

$$\boxed{\rightarrow P = \frac{506643}{\exp(55556 * r^2)} \ W/m^2}$$

For I-DEAS, the power intensity must be divided by the thickness, 0.375 inches (0.009525 m).

$$\rightarrow P = \frac{506643}{0.009525 * \exp(55556 * r^2)}$$

$$\rightarrow P = \frac{53{,}190{,}866}{\exp(55556 * r^2)} \ W/m^3$$

Verification (from I-DEAS):

```
Heat flow into sinks                = 2.866E+01
Heat flow from non-fluid sinks      = 0.000E+00
Heat load into elements             = 2.866E+01
Heat flow from fluid sinks          = 0.000E+00
Deviation from heat balance         = 4.387E-05
```

### B. Surface Heat Loads

There are three superimposed surface heat loads, which are applied in the I-DEAS model to a circular surface with radius 0.012 m. The loads are shown in the table below:

| **Pav (W)** | **ω (m)** | **$\omega^2$ ($m^2$)** |
|---|---|---|
| 3.3 | 0.006 | 0.000036 |
| 10 | 0.0032 | 0.00001024 |
| 1 | 0.00214 | 0.0000045796 |
| 14.3 | TOTAL | |

$$\rightarrow P = \frac{2*3.3}{\pi*0.000036*\exp(\frac{2r^2}{0.000036})} + \frac{2*10}{\pi*0.00001024*\exp(\frac{2r^2}{0.00001024})} + \frac{2*1}{\pi*0.0000045796*\exp(\frac{2r^2}{0.0000045796})}$$

$$\boxed{\rightarrow P = \frac{58357}{\exp(55556*r^2)} + \frac{621699}{\exp(195313*r^2)} + \frac{139012}{\exp(436719*r^2)} \quad W/m^2}$$

This function is shown graphically in Figure 1.

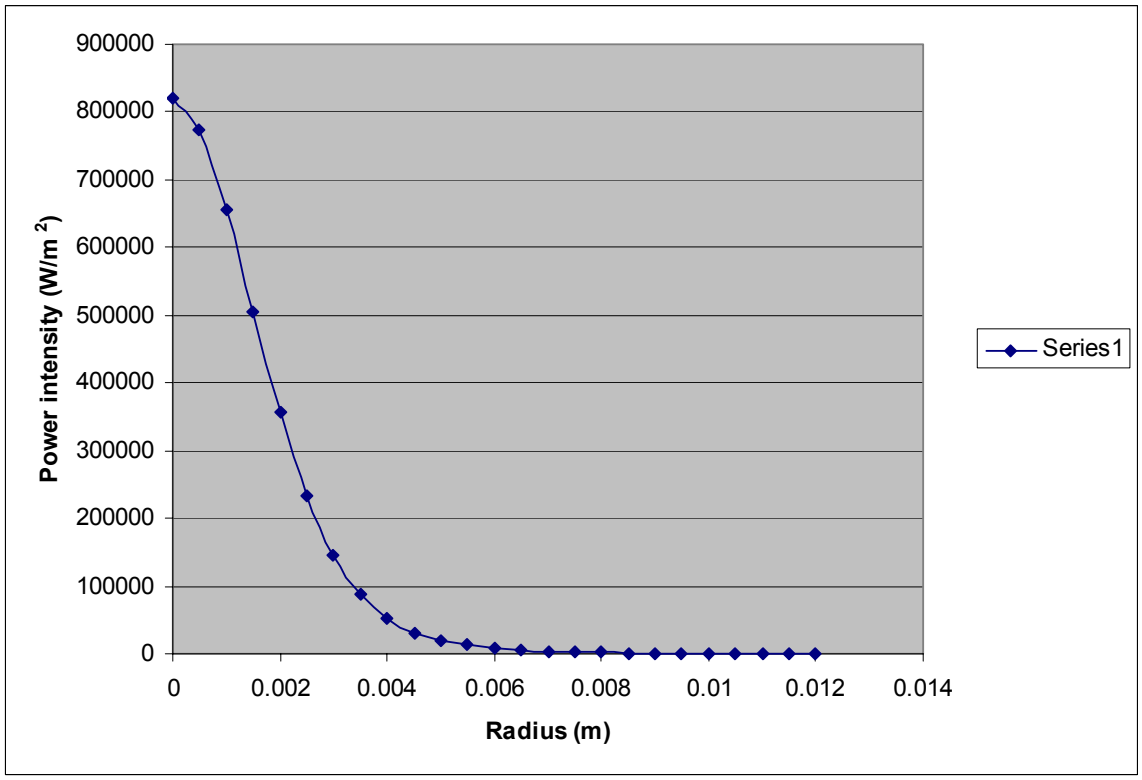


Figure 1: Power intensity (surface component only) as a function of radial distance from the center of the mirror

Verification (from I-DEAS):

```
Heat flow into sinks                = 1.430E+01
Heat flow from non-fluid sinks      = 0.000E+00
Heat load into elements             = 1.430E+01
Heat flow from fluid sinks          = 0.000E+00
Deviation from heat balance         = 9.537E-07
```

## II. Model Construction

The mirror is 2 inches in diameter and 0.375 inches thick. The mirror is meshed with solid parabolic tetrahedron elements, and the coolant is represented by beam elements with a cross section equal to that of the cooling channels.

The following assumptions were made in constructing the model:

1. That the contact between the solid materials was perfect (i.e., without gaps). This may not be correct, as the indium braze may have gaps where it is in contact with the surrounding surfaces.
2. That the coolant fluid conducts heat from all surrounding surfaces.
3. That all heat loads are essentially negligible beyond a radius of 12 mm and can be ignored after this radius.

Application of the bulk and surface heat loads is discussed above. The profile of the surface heat load is shown by the red data surface in Figure 2.

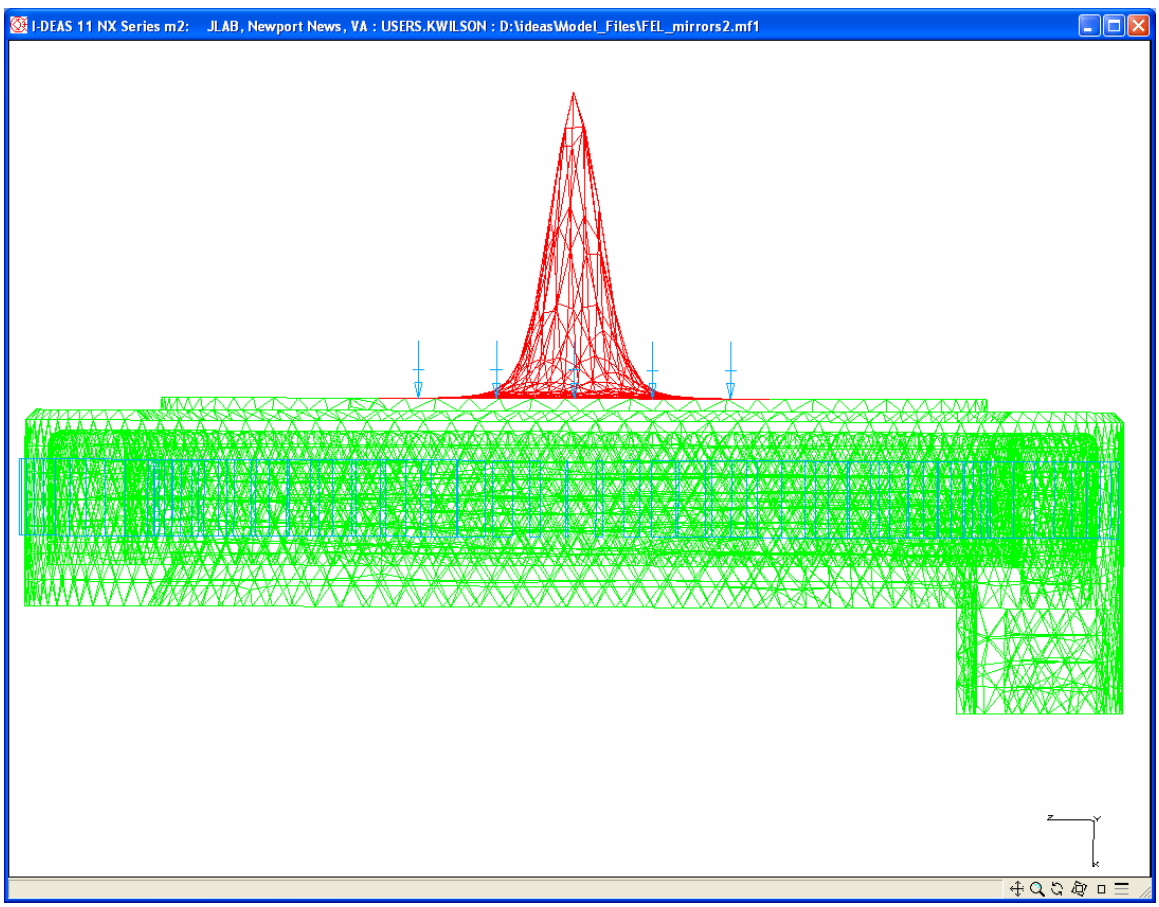


Figure 2: Surface heat load

The model consists of three solid materials, sapphire, indium and either niobium or molybdenum, plus a gas cooling fluid, either nitrogen or helium. Temperature-dependent thermal conductivities and coefficients of thermal expansion, given in section III, were

used for all. In Figure 3, yellow is the sapphire, dark blue is the indium and red is the niobium or molybdenum. The light blue rectangular elements are the coolant, whose properties are described in section IV.

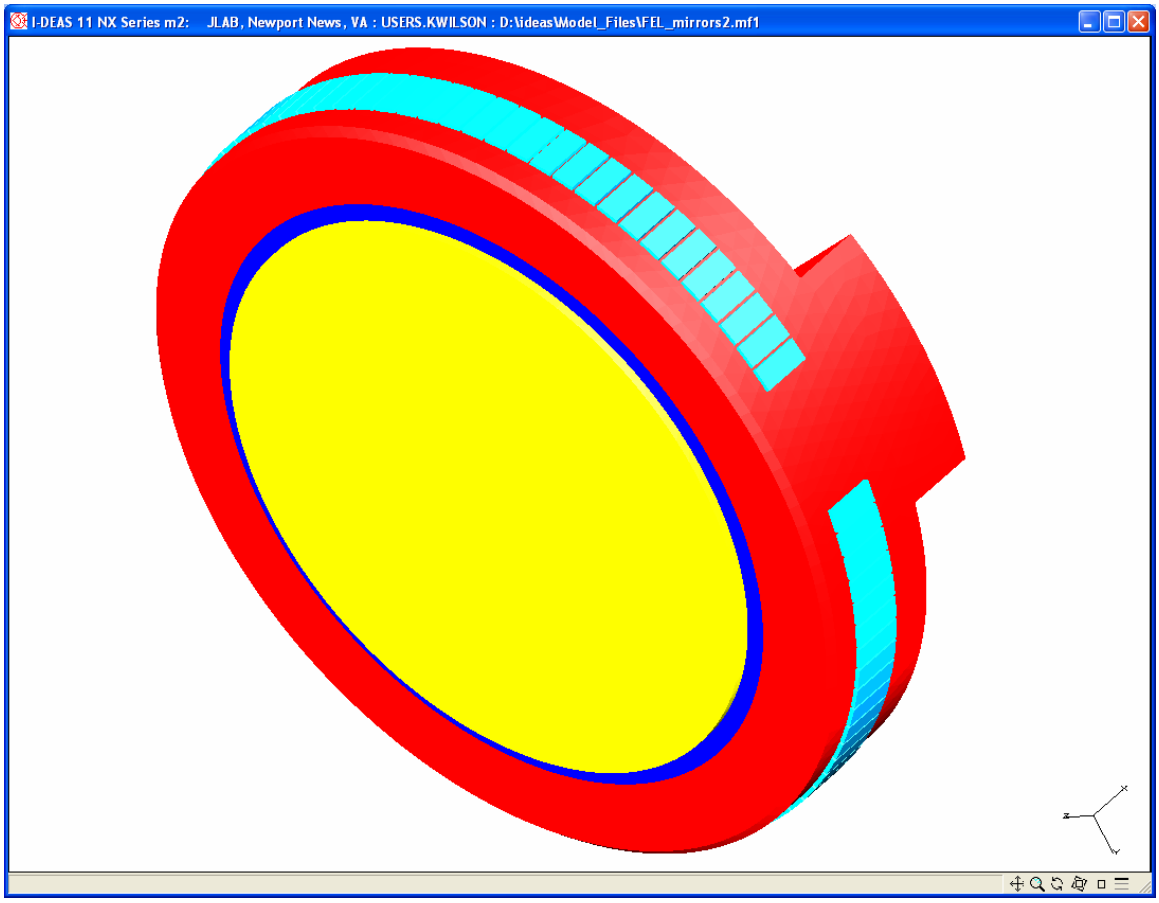


Figure 3: Finite element model of mirror showing materials

## III. Solid Material Properties

### A. Sapphire

Mechanical and thermal properties of sapphire are shown below.

| Temperature (K) | Thermal Conductivity (J/m/K/s) |
|---|---|
| 33 | 15000 |
| 44.2 | 7000 |
| 50 | 5000 |
| 53.8 | 4000 |
| 60.6 | 3000 |
| 65.4 | 2000 |
| 78.8 | 1000 |
| 88.5 | 600 |

| | |
|---|---|
| 100 | 400 |
| 300 | 94 |

Source: Bill Chronis up to 100 K, Table provided by Bill Chronis above 100 K

| Temperature (K) | Coefficient of Thermal Expansion (1/K) |
|---|---|
| 0 | 4.54 E-07 |
| 50 | 5.45 E-07 |
| 100 | 1.32 E-06 |
| 150 | 2.73 E-06 |
| 300 | 6 E-06 |

Source: Bill Chronis up to 150 K, graph provided by Bill Chronis above 100 K

Although thermal conductivity and coefficient of thermal expansion vary with the axis direction for sapphire, the table and graph from which this information was taken did not provide the axis which the properties apply to.

Modulus of Elasticity 2.0 E+11 Pa
Poisson's Ratio 0.27

### B. Indium

Mechanical and thermal properties of indium are shown below.

| Temperature (K) | Thermal Conductivity (J/m/K/s) |
|---|---|
| 40 | 100 |
| 50 | 90 |
| 60 | 84 |
| 70 | 80 |
| 80 | 77 |
| 90 | 73 |
| 100 | 72 |
| 120 | 70 |
| 140 | 69 |
| 160 | 68 |
| 200 | 66 |
| 250 | 66 |
| 300 | 66 |

Source: Selected Cryogenic Data Notebook by Brookhaven National Laboratory

| Temperature (K) | Coefficient of Thermal Expansion (1/K) |
|---|---|
| 40 | 1.7 E-005 |
| 50 | 1.91 E-005 |
| 60 | 2.04 E-005 |
| 70 | 2.15 E-005 |
| 80 | 2.24 E-005 |

| | |
|---|---|
| 90 | 2.23 E-005 |
| 100 | 2.39 E-005 |
| 120 | 2.52 E-005 |
| 140 | 2.63 E-005 |
| 160 | 2.72 E-005 |
| 200 | 2.86 E-005 |
| 260 | 3.08 E-005 |
| 300 | 3.22 E-005 |

Source: Selected Cryogenic Data Notebook by Brookhaven National Laboratory

Modulus of Elasticity 1.274 E+010 Pa
Poisson's Ratio 0.4498

### C. Niobium

Mechanical and thermal properties of niobium are shown below.

| Temperature (K) | Thermal Conductivity (J/m/K/s) |
|---|---|
| 40 | 74 |
| 50 | 65 |
| 60 | 58 |
| 70 | 54 |
| 80 | 52 |
| 90 | 51 |
| 100 | 51 |
| 120 | 50 |
| 300 | 50 |

Source: Selected Cryogenic Data Notebook by Brookhaven National Laboratory

| Temperature (K) | Coefficient of Thermal Expansion (1/K) |
|---|---|
| 40 | 1.7 E-06 |
| 50 | 2.4 E-06 |
| 60 | 3.1 E-06 |
| 70 | 3.6 E-06 |
| 80 | 4.0 E-05 |
| 90 | 4.4 E-06 |
| 100 | 4.7 E-06 |
| 120 | 5.2 E-06 |
| 160 | 5.9 E-06 |
| 200 | 6.4 E-06 |
| 260 | 6.8 E-06 |
| 300 | 7 E-06 |

Source: Selected Cryogenic Data Notebook by Brookhaven National Laboratory

Modulus of Elasticity 1.23416e+011
Poisson's Ratio 0.38

### D. Molybdenum

Mechanical and thermal properties of molybdenum are shown below.

| Temperature (K) | Thermal Conductivity (J/m/K/s) |
|---|---|
| 30 | 370 |
| 35 | 375 |
| 40 | 360 |
| 50 | 320 |
| 60 | 270 |
| 70 | 230 |
| 80 | 210 |
| 90 | 186 |
| 100 | 174 |
| 120 | 157 |
| 140 | 147 |
| 160 | 141 |
| 200 | 140 |
| 250 | 138 |
| 300 | 137 |
| 100 | 137 |

Source: Selected Cryogenic Data Notebook by Brookhaven National Laboratory

| Temperature (K) | Coefficient of Thermal Expansion (1/K) |
|---|---|
| 1 | 0 |
| 50 | 1 E-06 |
| 100 | 2.8 E-06 |
| 200 | 4.5 E-06 |
| 300 | 4.7 E-06 |

Source: Selected Cryogenic Data Notebook by Brookhaven National Laboratory

Modulus of Elasticity 1.1e+011
Poisson's Ratio 0.35

## IV. Coolant Properties

The flow rates for both gases were those suggested by Bill Chronis as optimal.

### A. Gas Nitrogen

Mass density 3.93 kg/m$^3$

| | |
|---|---|
| Specific heat at constant pressure | 1000 J/kg/K |
| Dynamic viscosity | 5.26839 E-06 kg/m/s |
| Gas constant | 290 J/kg/K |

| Temperature (K) | Thermal Conductivity (J/m/K/s) |
|---|---|
| 77.36 | 0.757 |
| 80.00 | 0.782 |
| 90.00 | 0.873 |

Source: Bill Chronis

| | |
|---|---|
| Mass flow rate | 0.01 kg/s |
| Inlet pressure | 1.75 atm |
| Inlet temperature | 80 K |

### B. Gas Helium

| | |
|---|---|
| Mass density | 4.53 kg/m$^3$ |
| Specific heat at constant pressure | 5243 J/kg/K |
| Dynamic viscosity | 5.6 E-06 kg/m/s |
| Gas constant | 2077 J/kg/K |

The thermal conductivity table shown below is an abbreviated version for the purposes of conserving space.

| Temperature (K) | Thermal Conductivity (J/m/K/s) |
|---|---|
| 40 | 0.0412 |
| 60 | 0.053 |

Source: Bill Chronis

| | |
|---|---|
| Mass flow rate | 0.02 kg/s |
| Inlet pressure | 3.75 atm |
| Inlet temperature | 40 K |

## V. Results

Thermal results of the analyses are shown below. Results are shown for several cases. Initially, a model with a niobium holder was used, and both gas helium and gas nitrogen cooling fluids were evaluated. Based on these results, nitrogen was discarded and only helium was used for cooling. The niobium was also replaced with molybdenum in an attempt to minimize the thermal stresses in the part.

All temperatures are shown in Kelvin

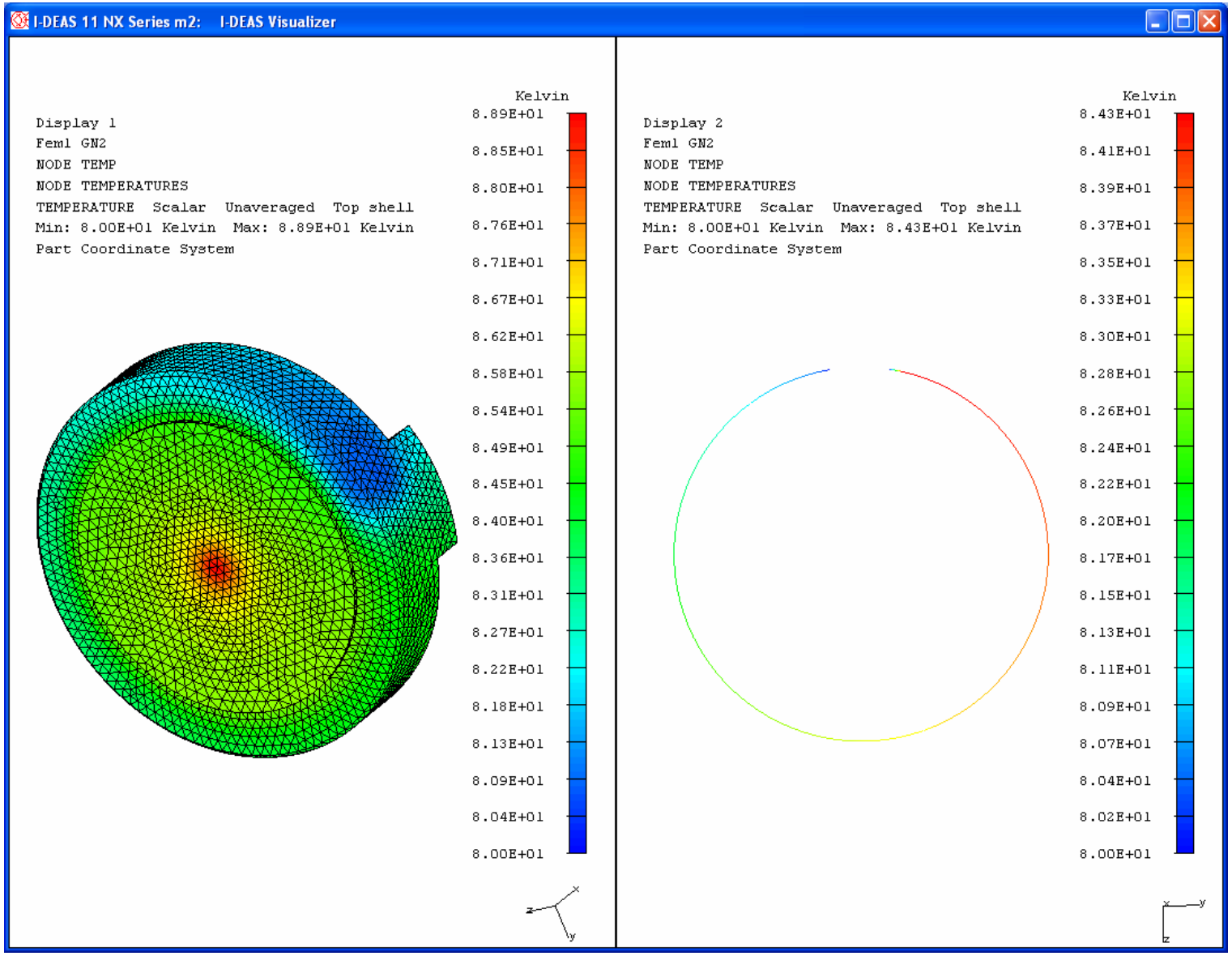

Figure 4: Thermal profile, GN2 cooling, niobium holder; part temperatures on left and gas temperatures on right

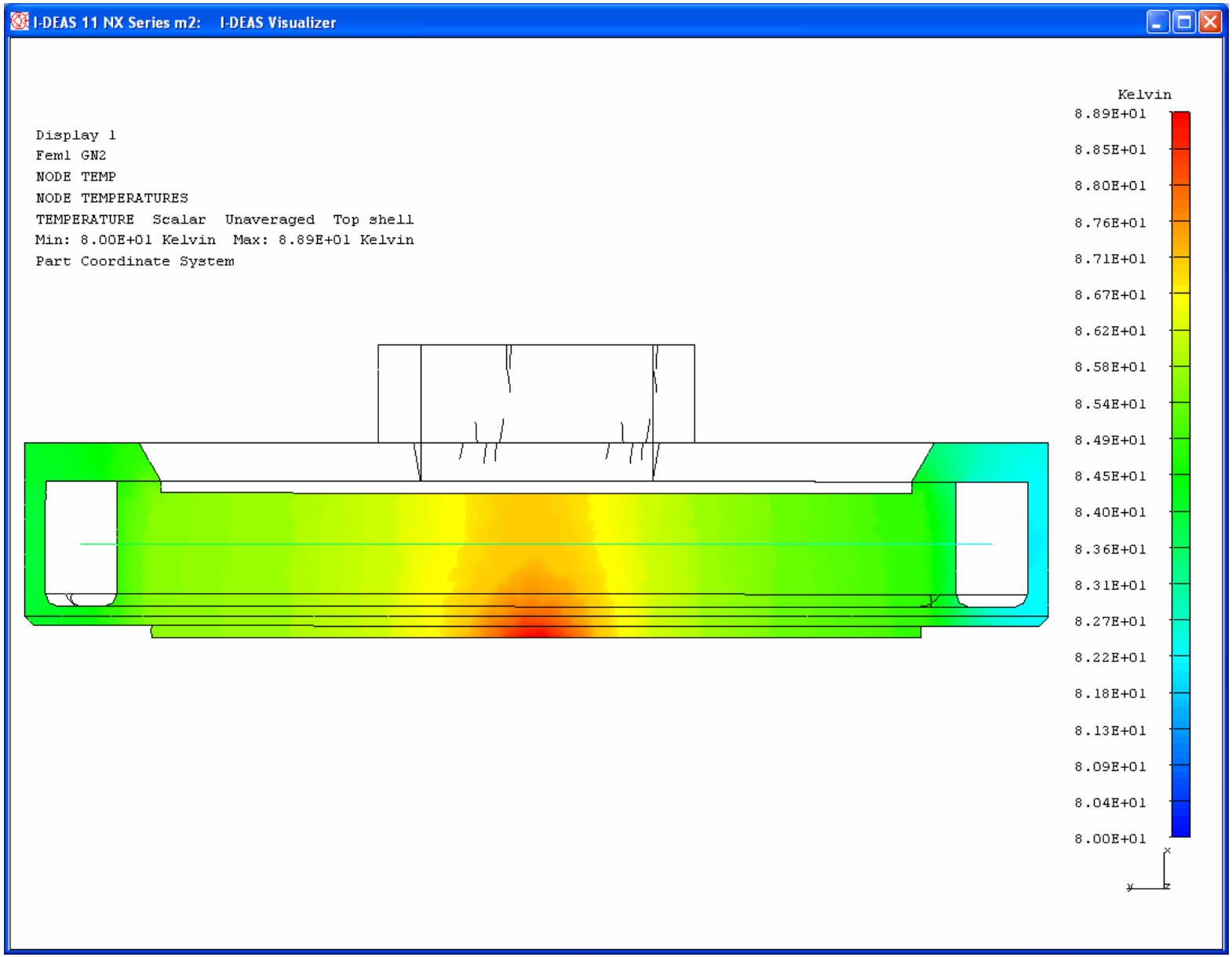

Figure 5: Thermal cross-section, GN2 cooling, niobium holder

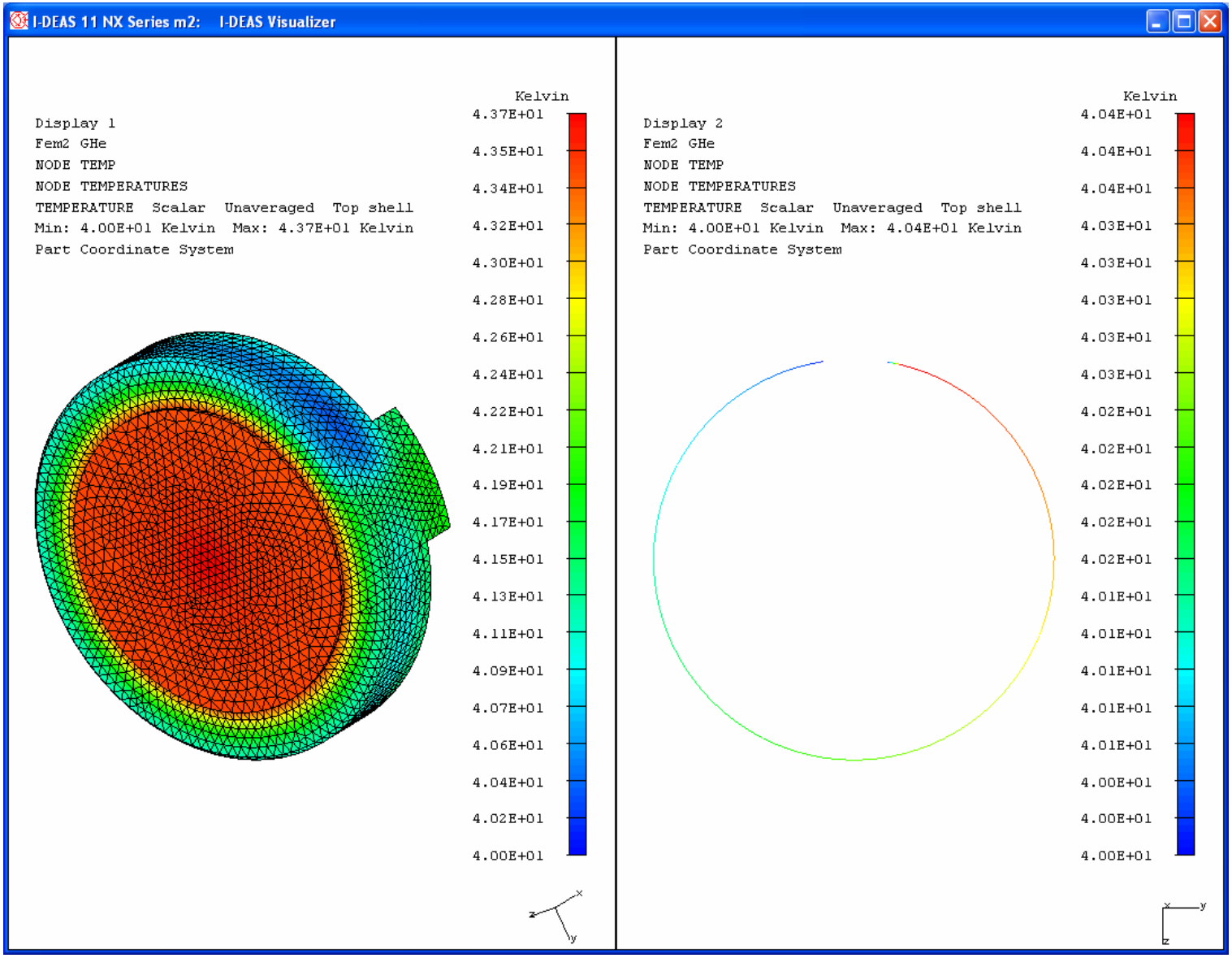

Figure 6: Thermal profile, GHe cooling, niobium holder; part temperatures on left and gas temperatures on right

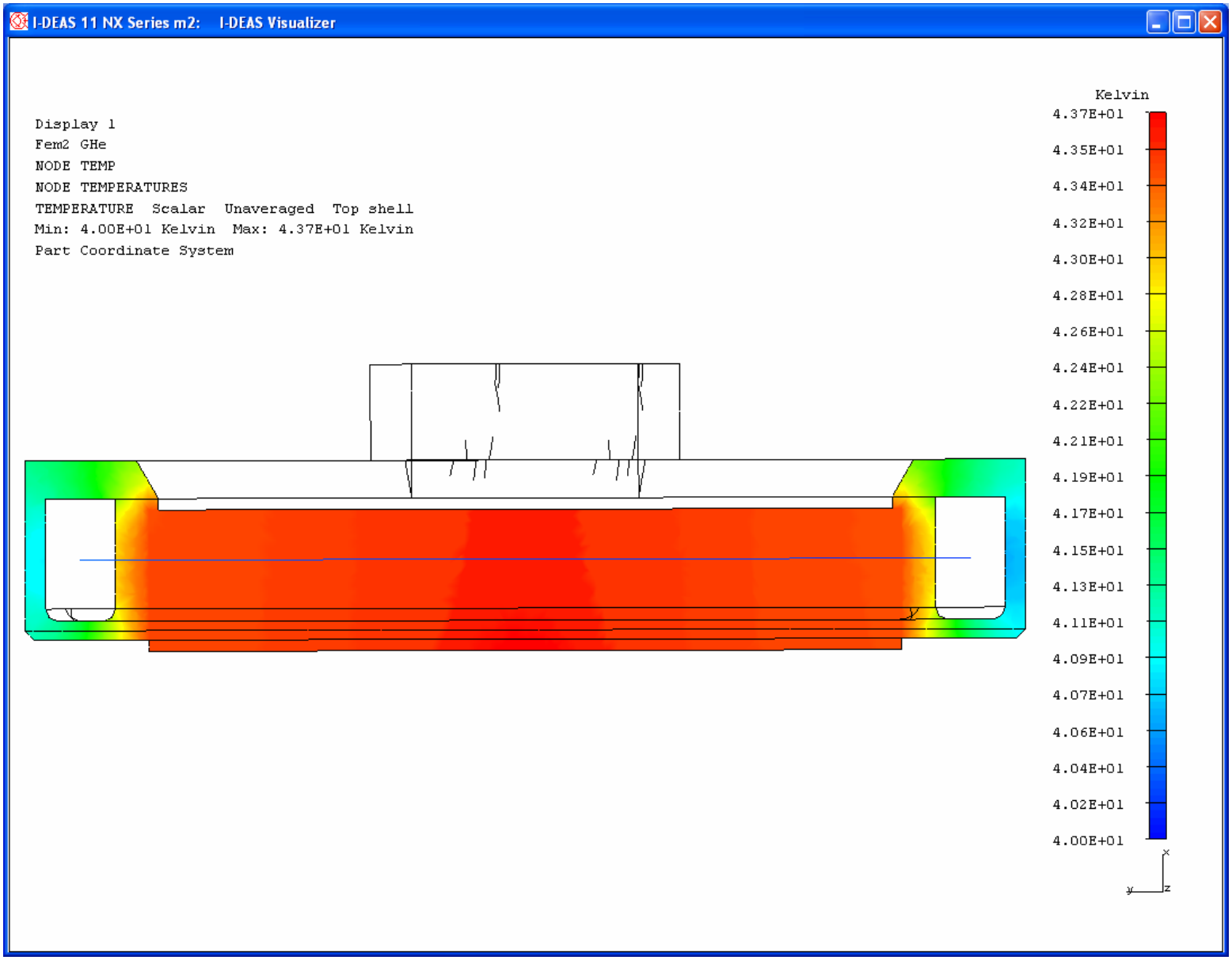

Figure 7: Thermal cross-section, GHe cooling, niobium holder

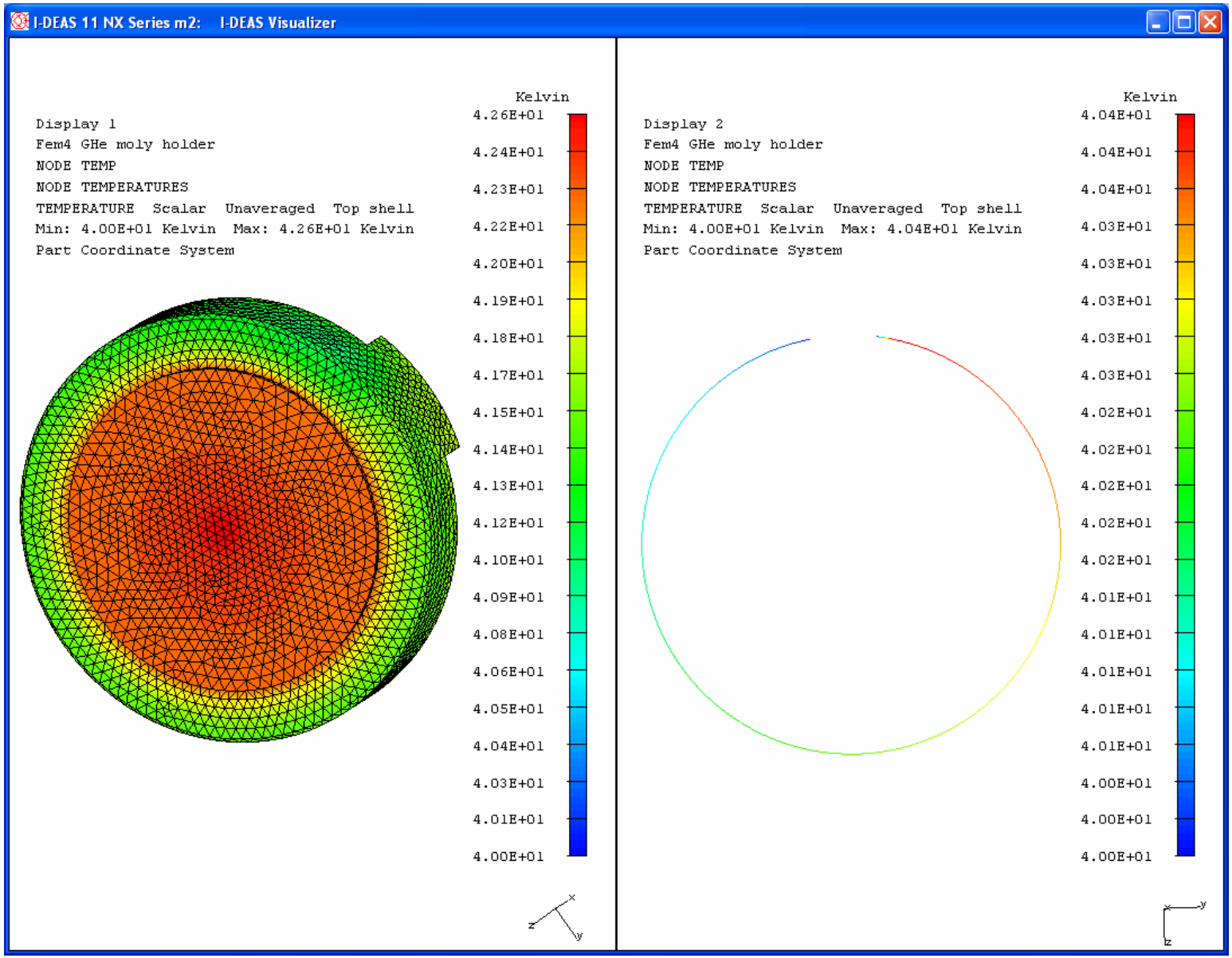

Figure 8: Thermal profile, GHe cooling, molybdenum holder; part temperatures on left and gas temperatures on right

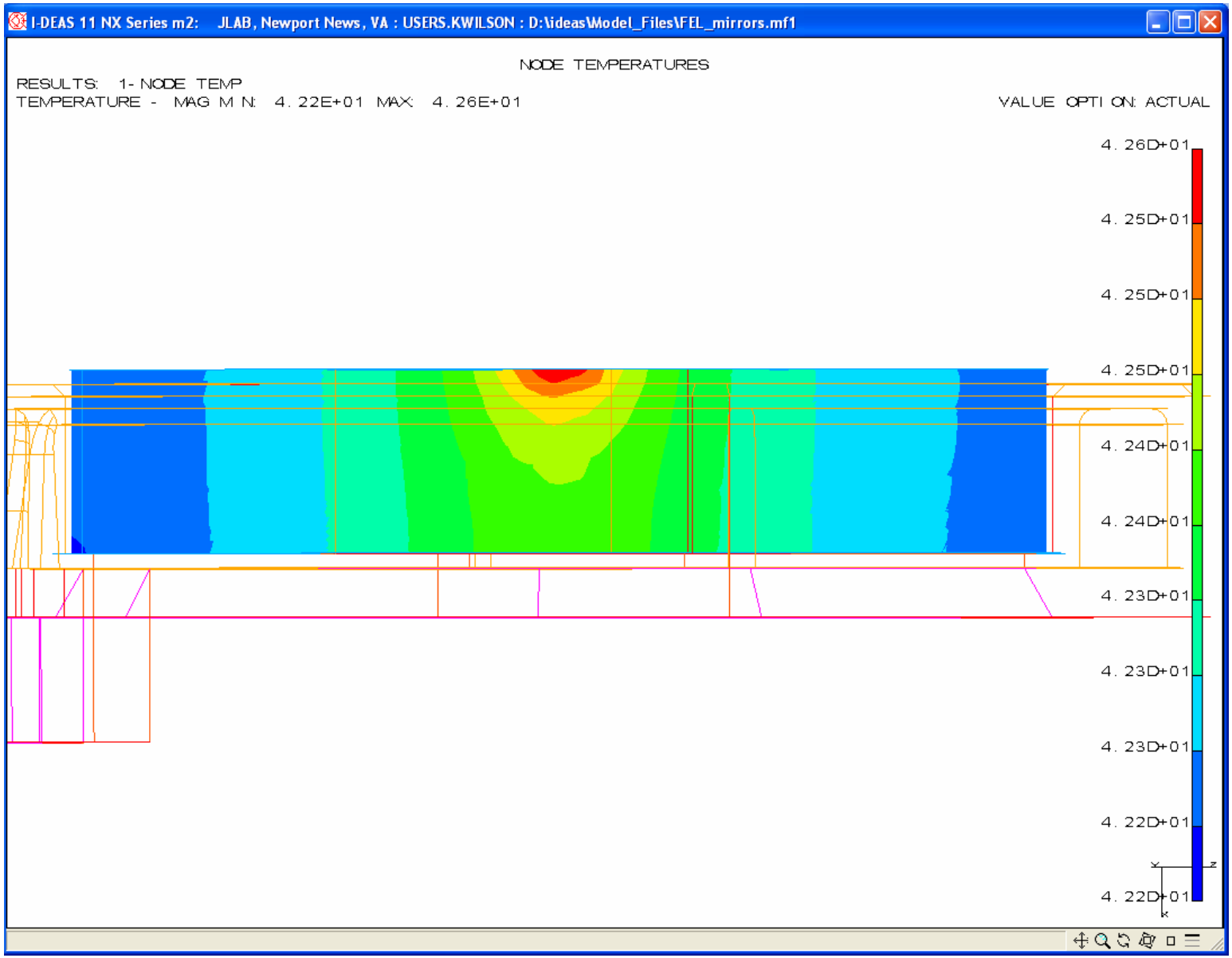

Figure 9: Thermal cross-section of mirror only, GHe cooling, molybdenum holder

## VI. Stress/Deflection Analysis

The thermal stresses and deflections resulting from the temperature profiles above were calculated.

The temperatures generated by the thermal model were transferred to the nodes of the stress analysis.

The model was also fixed at several locations. The centerpoint of the front face of the model was restrained in the radial direction to prevent free body motion. This permits the model to expand and contract about the centerpoint. In addition, three nodes on the front face of the model were restrained in the axial direction. These represent the location of the pins which keep the mirror assembly in the holder. These are shown in Figure 10.

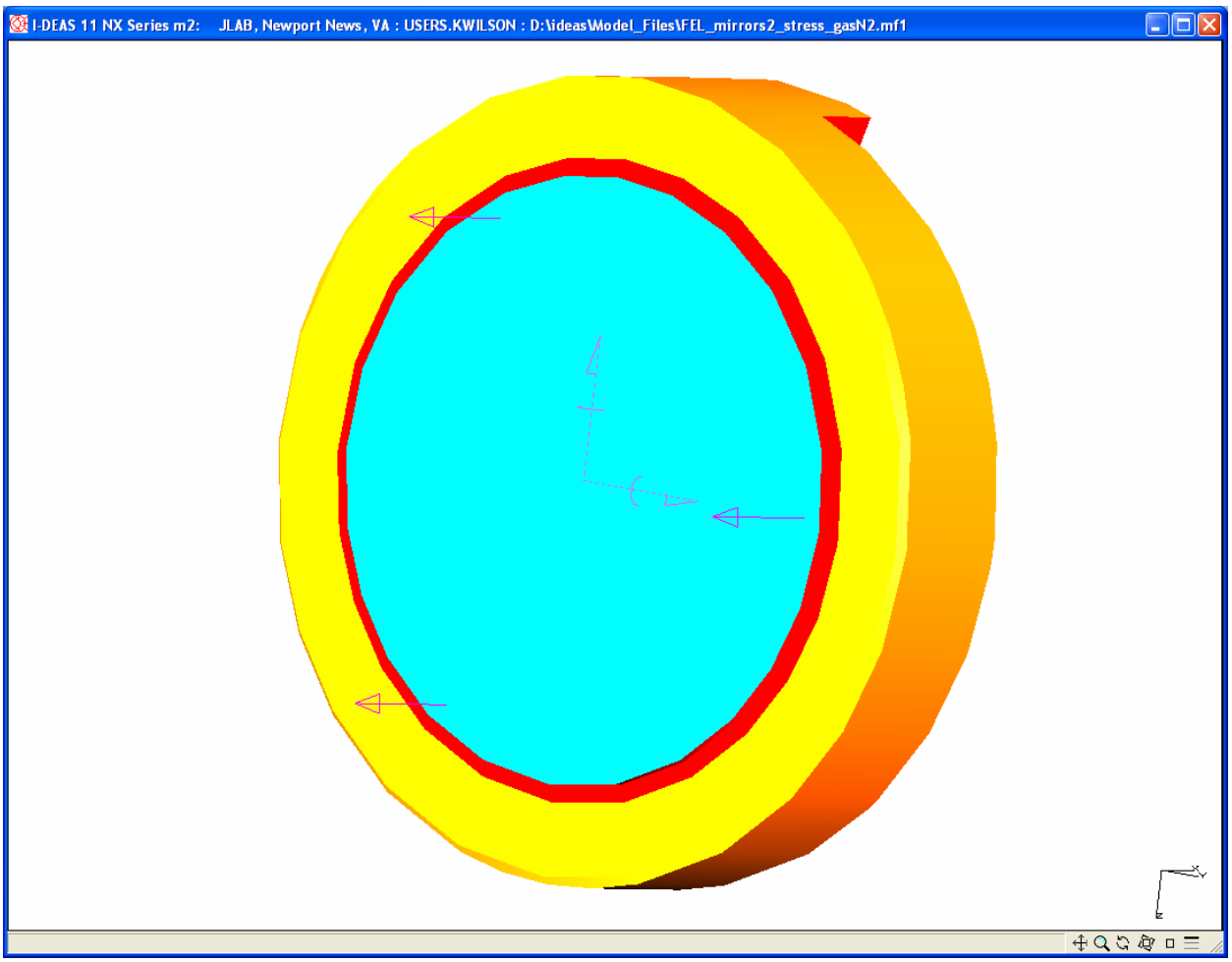


Figure 10: Restraints on mechanical model

The initial temperature of the model was 40 K for the gas helium case and 80 K for the gas nitrogen case. I-DEAS calculated the stresses and deflections resulting from the change from the initial temperature to the final temperature profile determined during the thermal analysis. Results are shown below.

All figures below show the model with a niobium holder except for the last figure which has a molybdenum holder. Although the original design had a niobium holder, due to the high stresses generated during cool-down, a molybdenum holder was considered as an option.

All stress results are in Pascals and all displacement results are in meters.

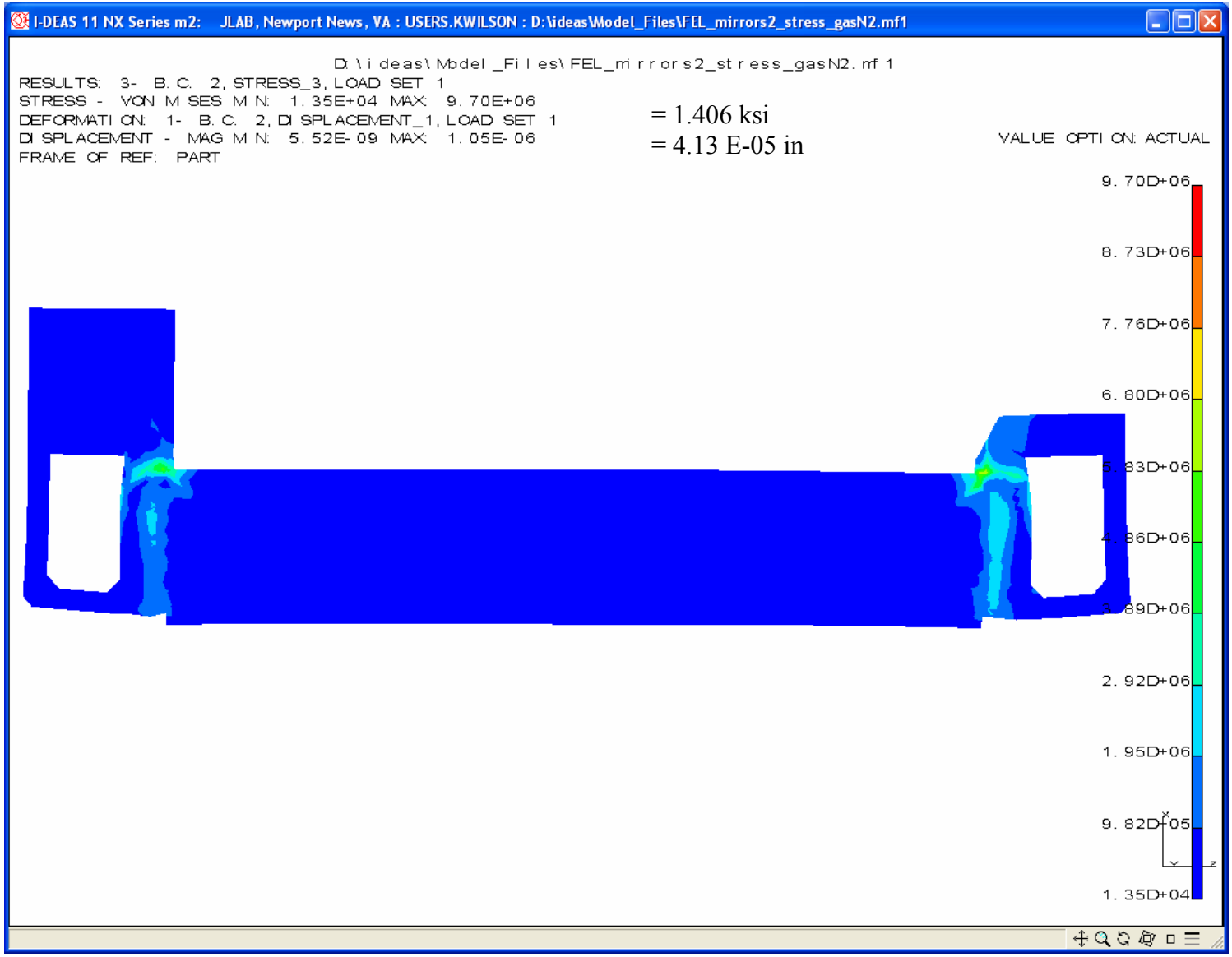


Figure 11: Von Mises stresses and displacement magnitudes, GN2, Nb holder, temperature from 80K to final temperature profile

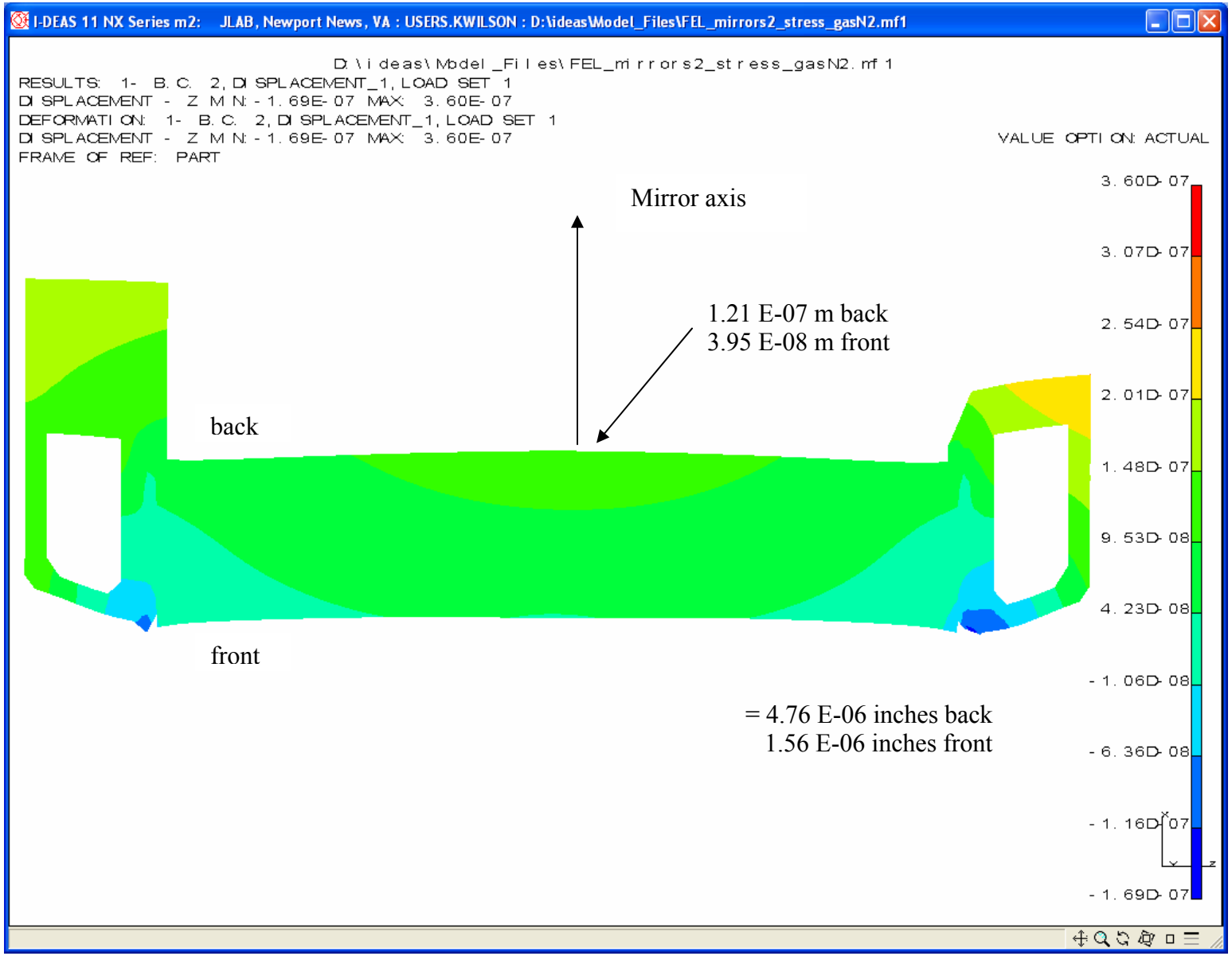


Figure 12: Displacements along axis, GN2, Nb holder, temperature from 80K to final temperature profile

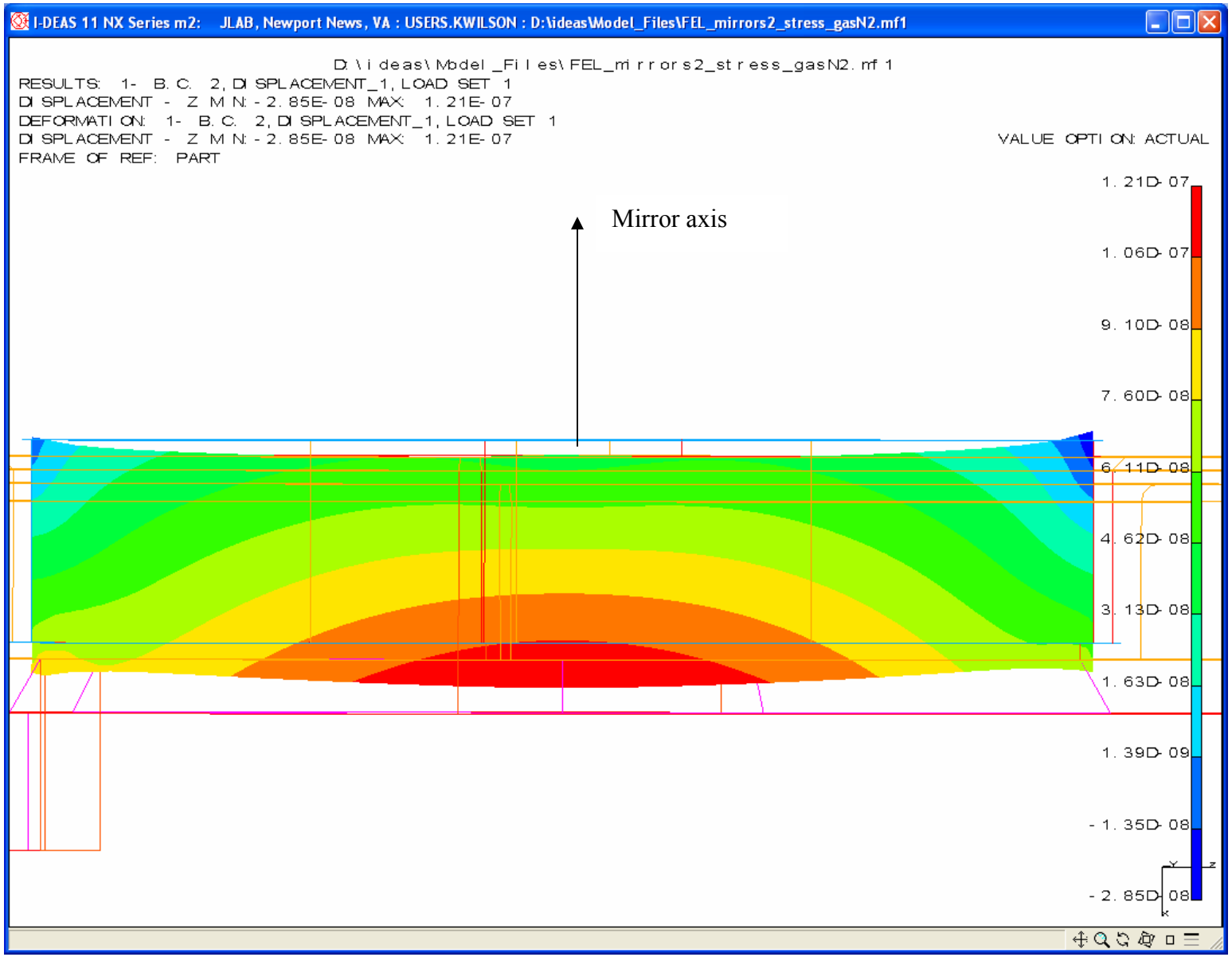

Figure 13: Displacements along axis, GN2, Nb holder,temperature from 80K to final temperature profile

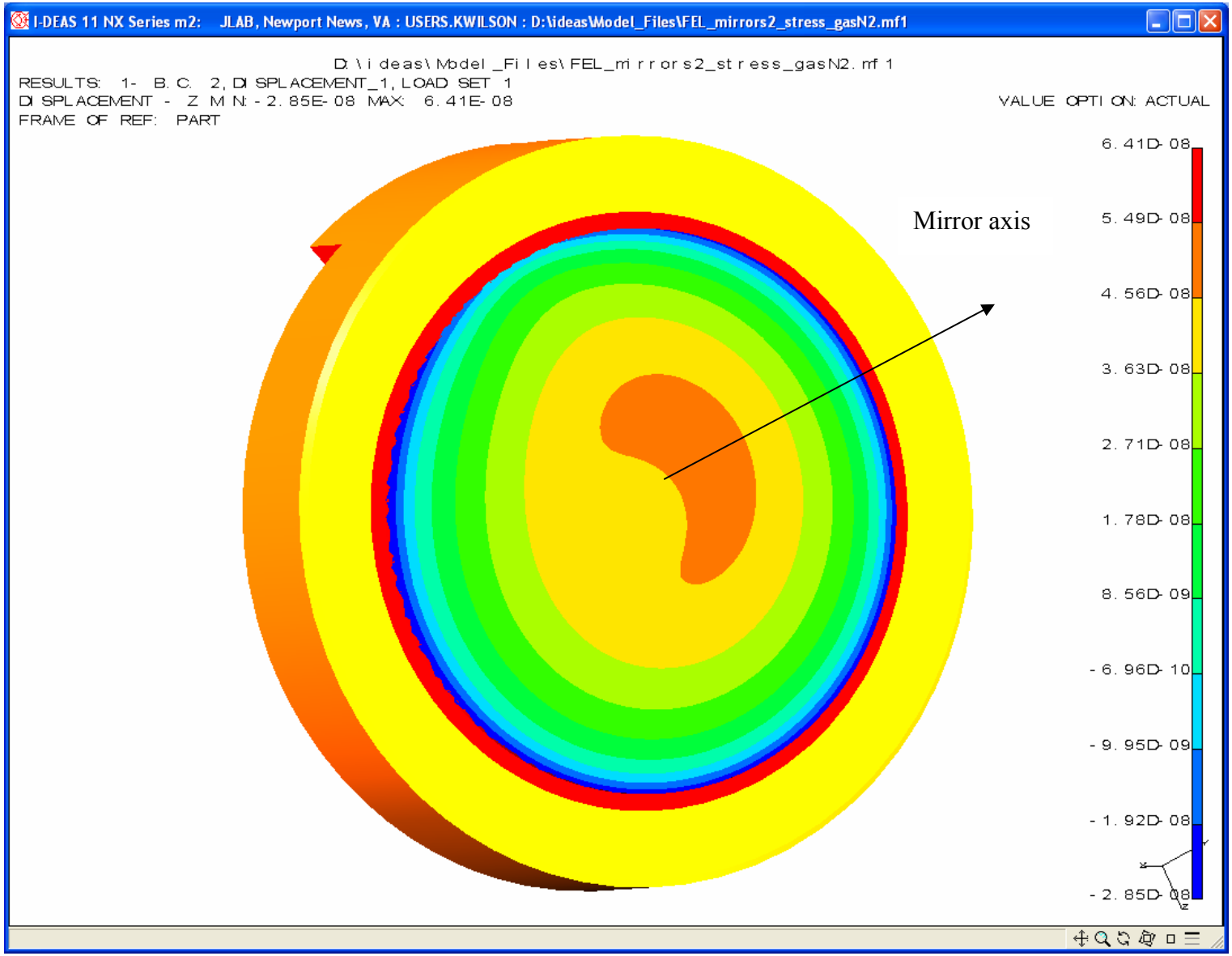

Figure 14: Displacements along axis, GN2, Nb holder, temperature from 80K to final temperature profile

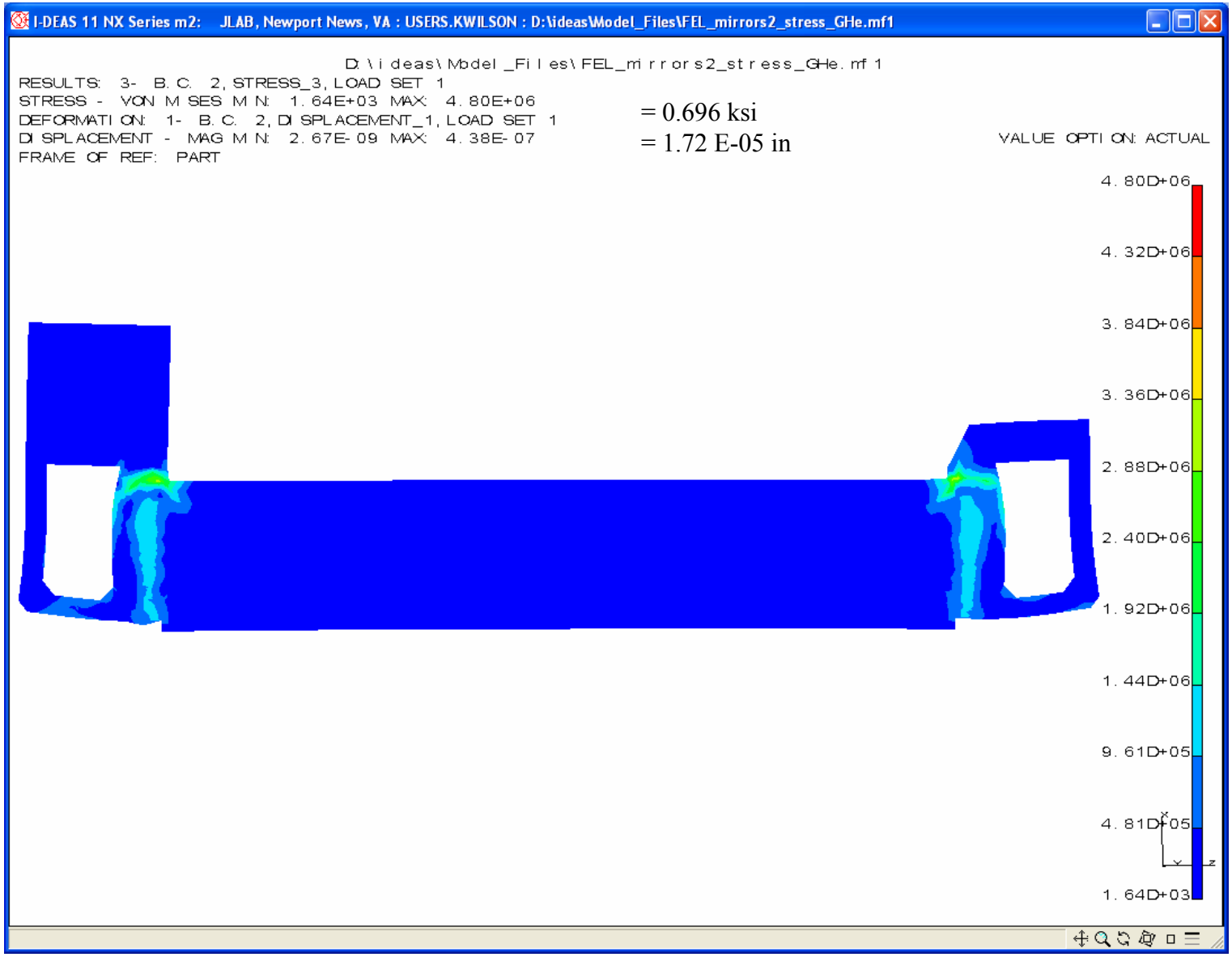


Figure 15: Von Mises stresses and displacement magnitudes, GHe, Nb holder, temperature from 40K to final temperature profile

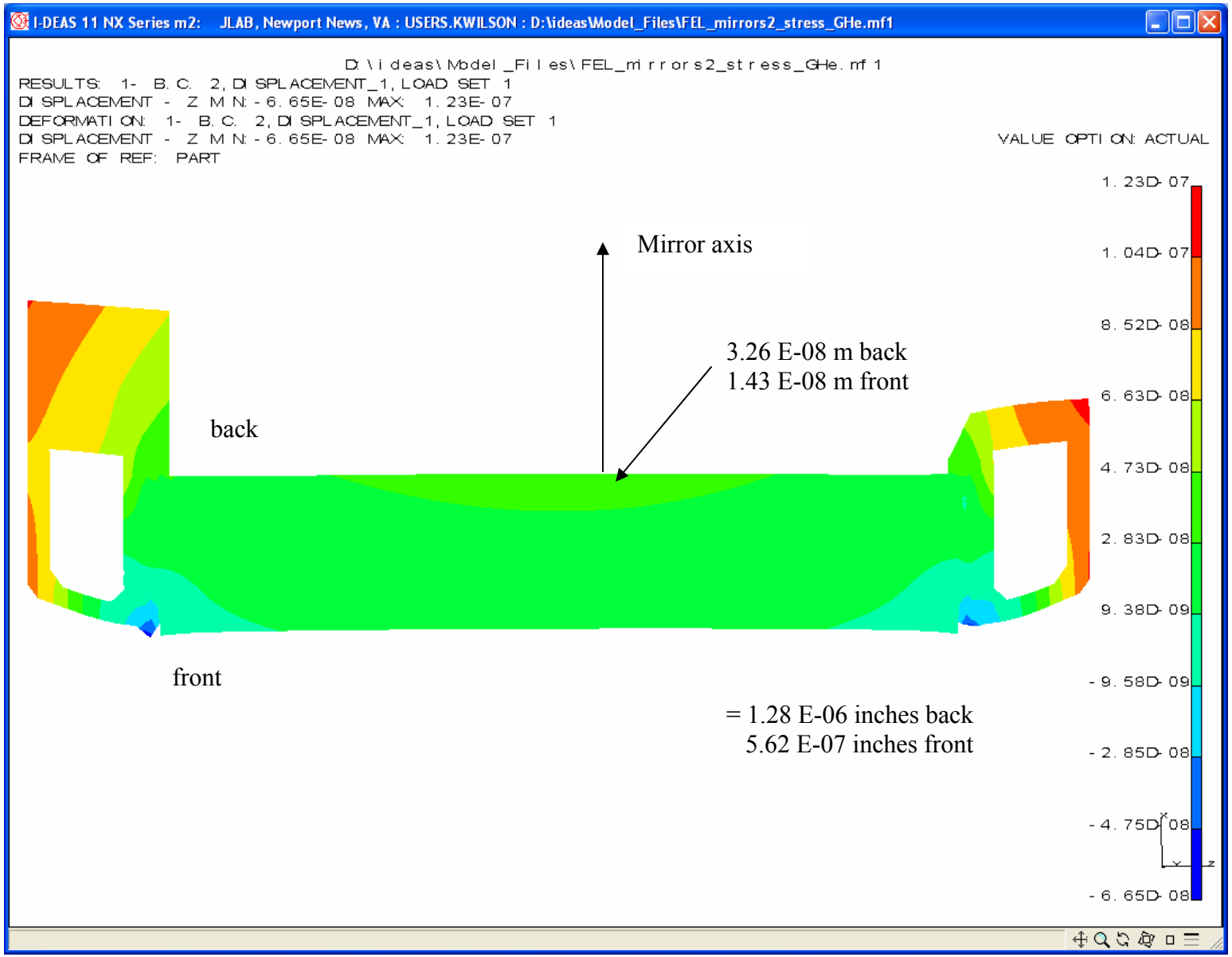


Figure 16: Displacements along axis, GHe cooling, Nb holder, temperature from 40K to final temperature profile

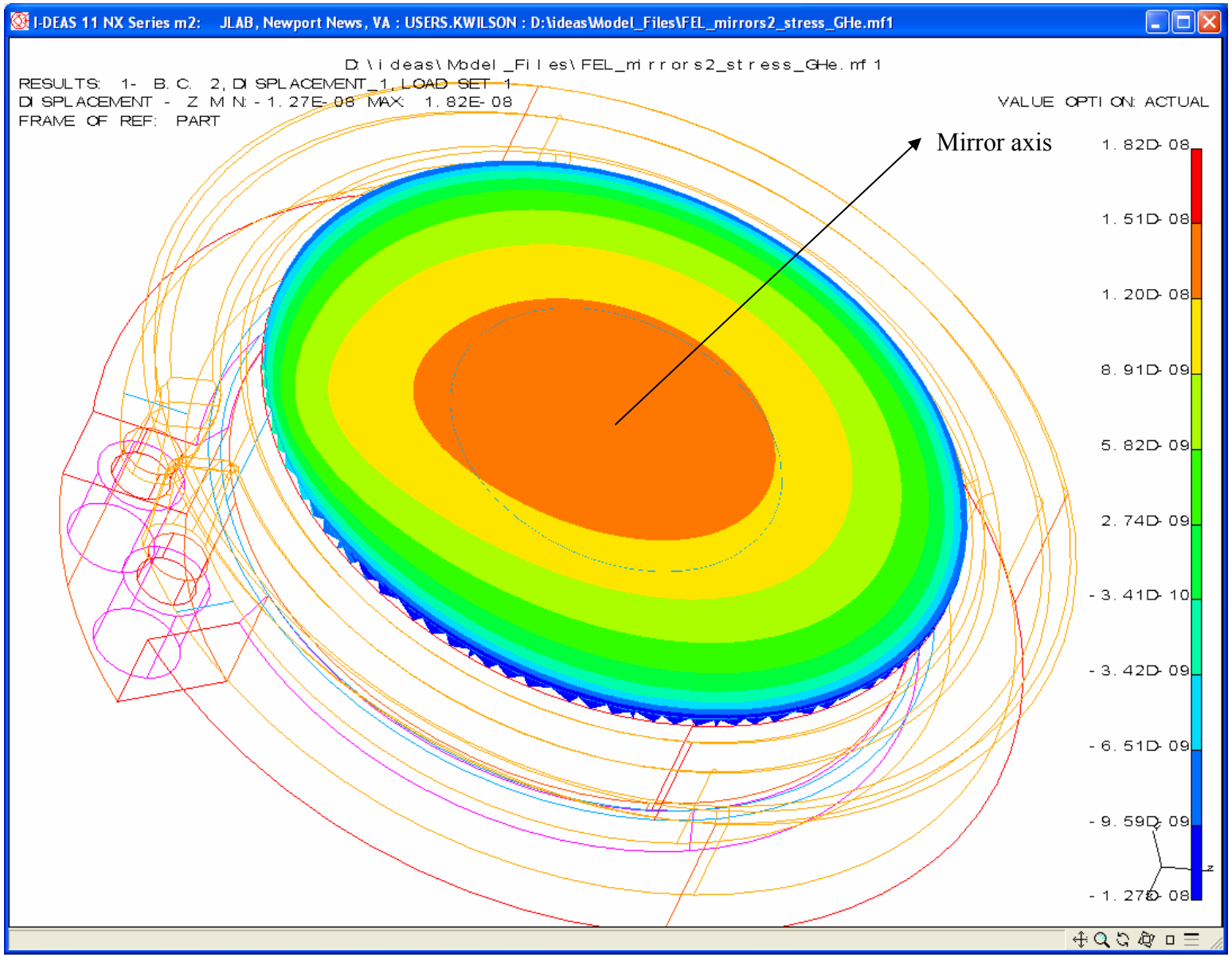


Figure 17: Displacements of front surface along axis, GHe cooling, Nb holder, temperature from 40K to final temperature profile

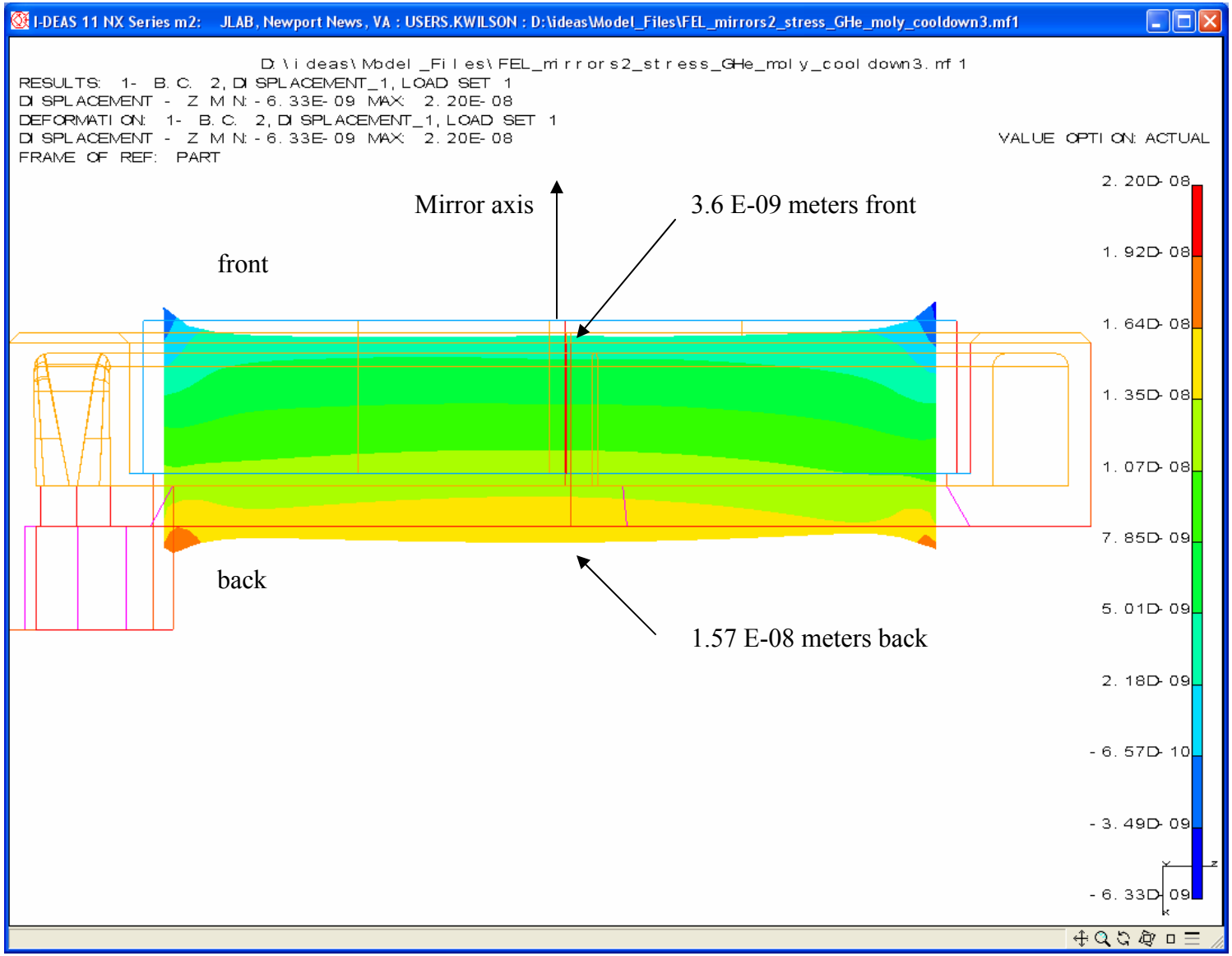


Figure 18: Cross-section of mirror: displacements along axis, GHe, molybdenum holder, temperature from 40K to final temperature profile

Finally, the cool-down stresses were evaluated for the different configurations. For these cases, the model was initially set to 300K and then cooled down to the final temperature profile. Although combining the effects of cool-down and heating slightly minimizes the thermal stresses (because the model of the mirror is cooled from 300 K to just over 40 K rather than to exactly 40 K), this method of modeling does show the thermal deformations that would be expected to affect mirror operations.

Figures 23 and 24 show the displacements in the mirror alone, without a holder, resulting from the cooldown.

For these results, only the cases with GHe cooling are shown.

All distance measurements are given in meters.

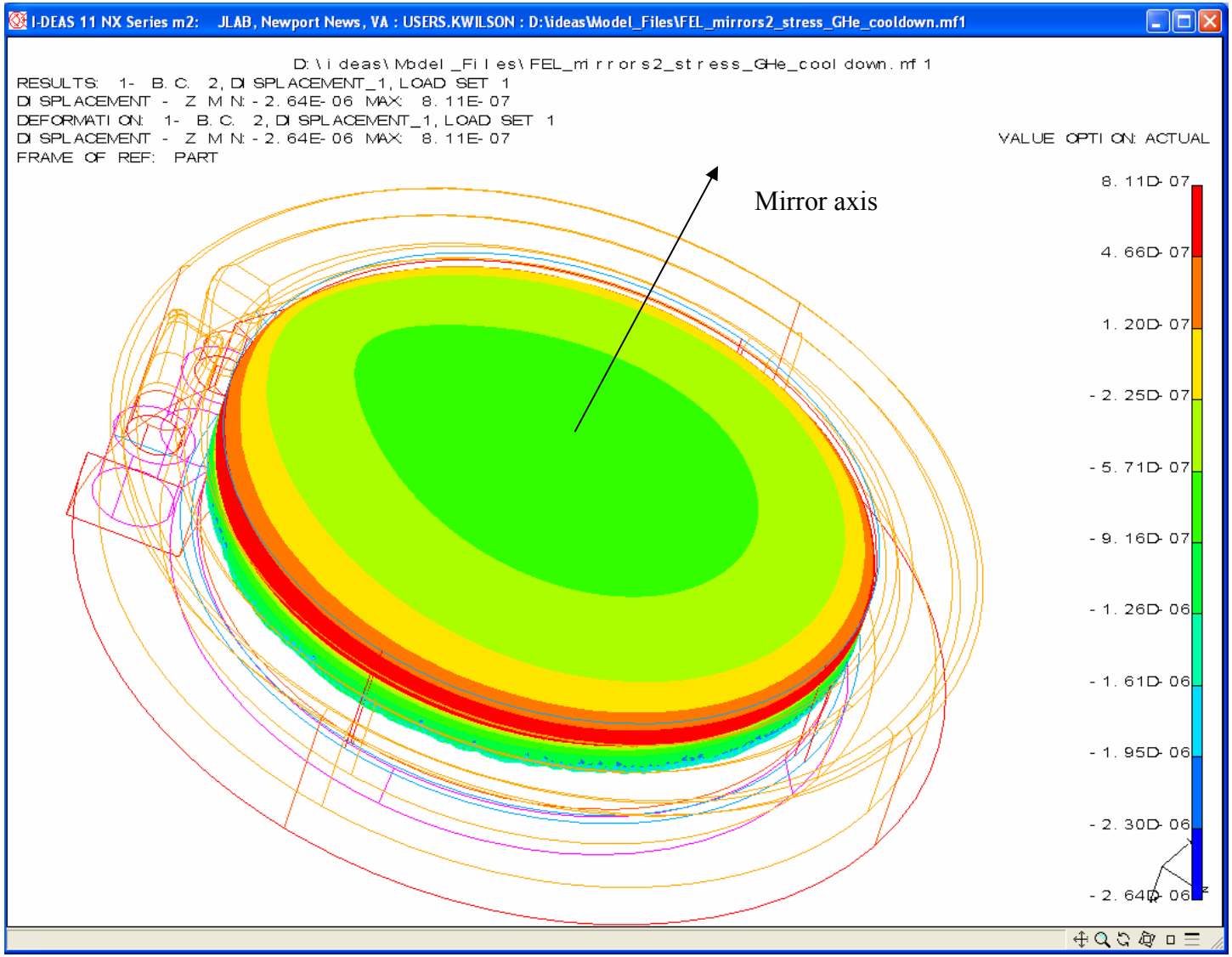


Figure 19: Displacements of front surface along axis of mirror, GHe cooling, Nb holder, temperature from 300K to final temperature profile

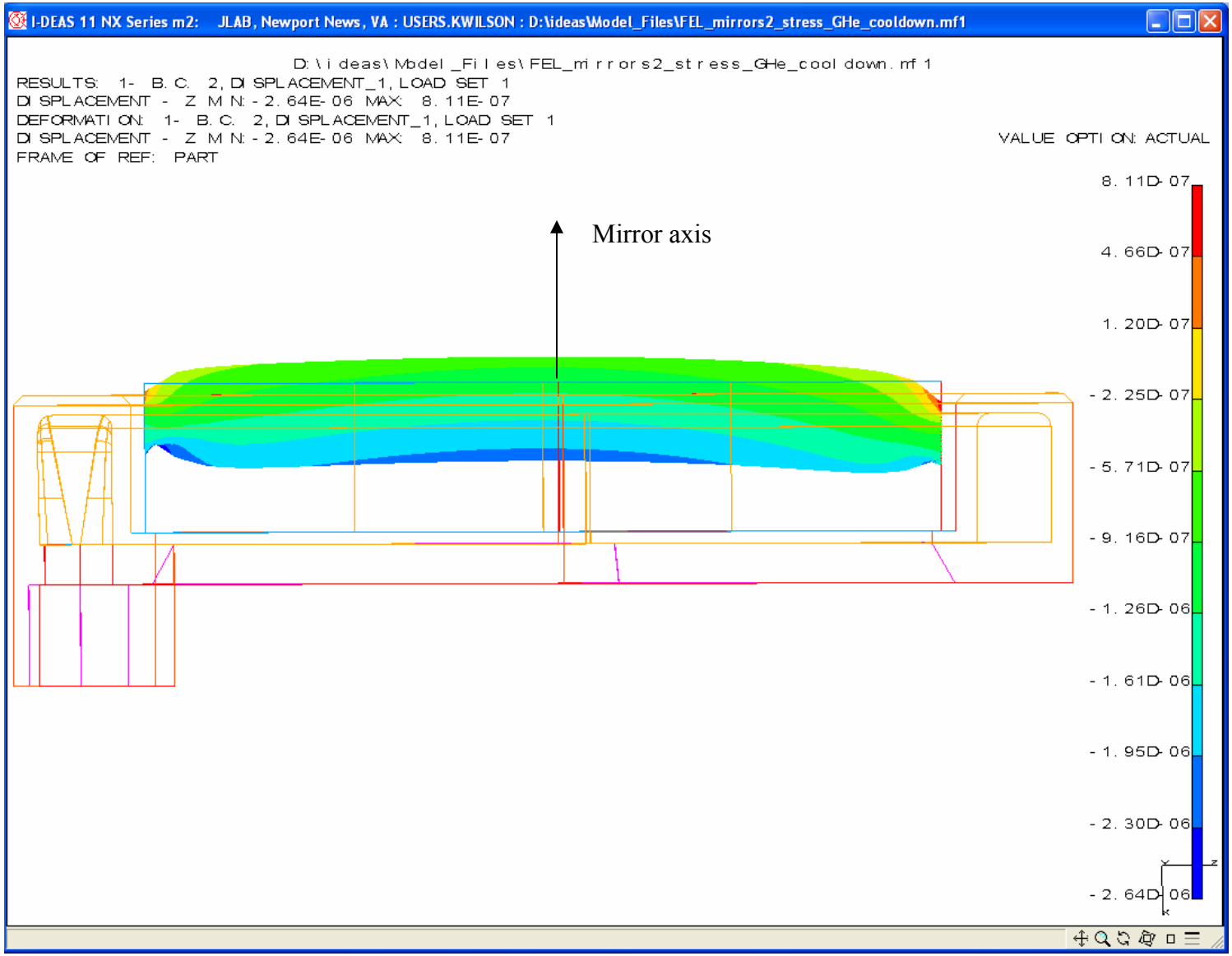

Figure 20: Displacements of cross-section along mirror axis, GHe, Nb holder, temperature from 300K to final temperature profile

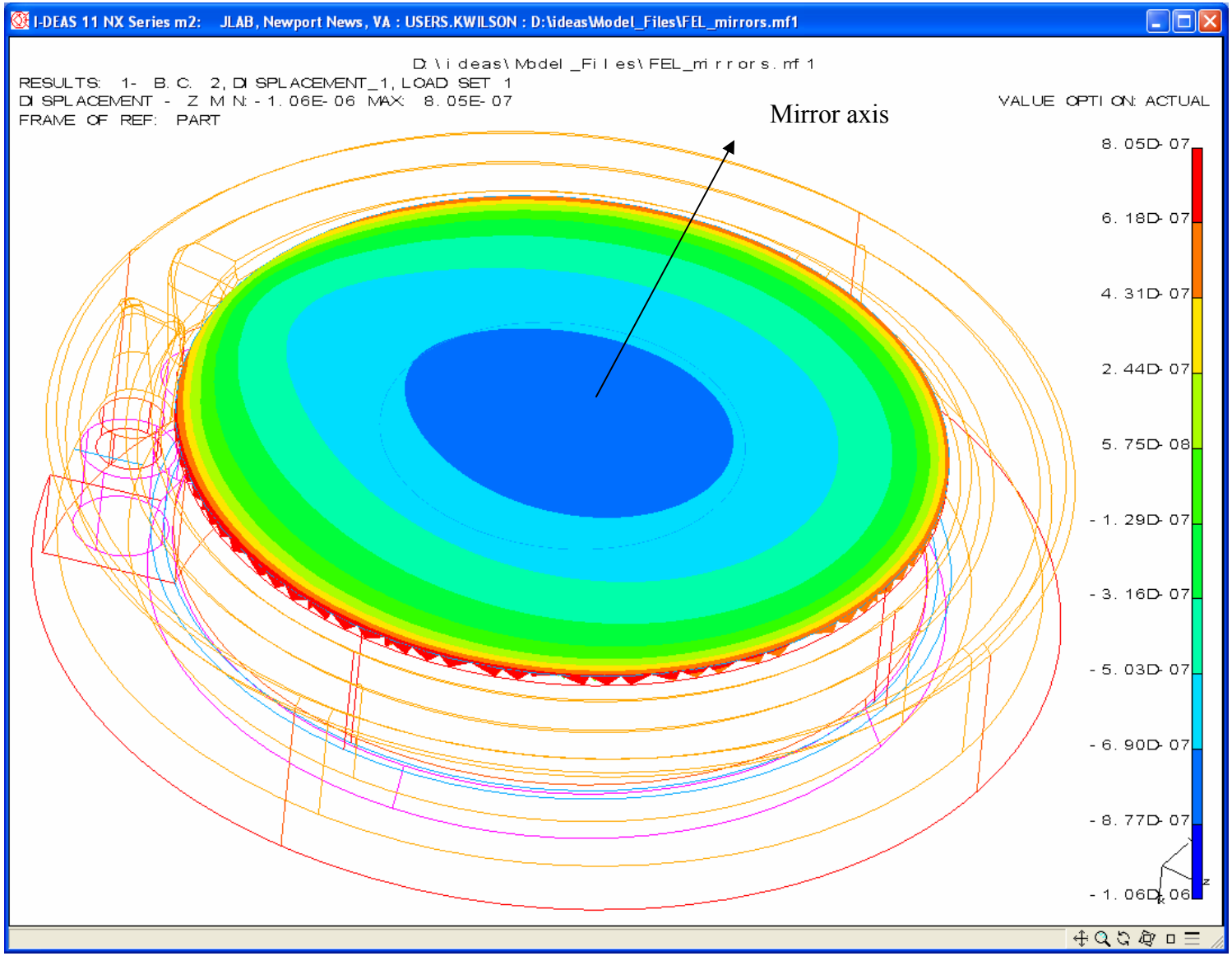


Figure 21: Displacements of cross-section along mirror axis, GHe, molybdenum holder, temperature from 300K to final temperature profile

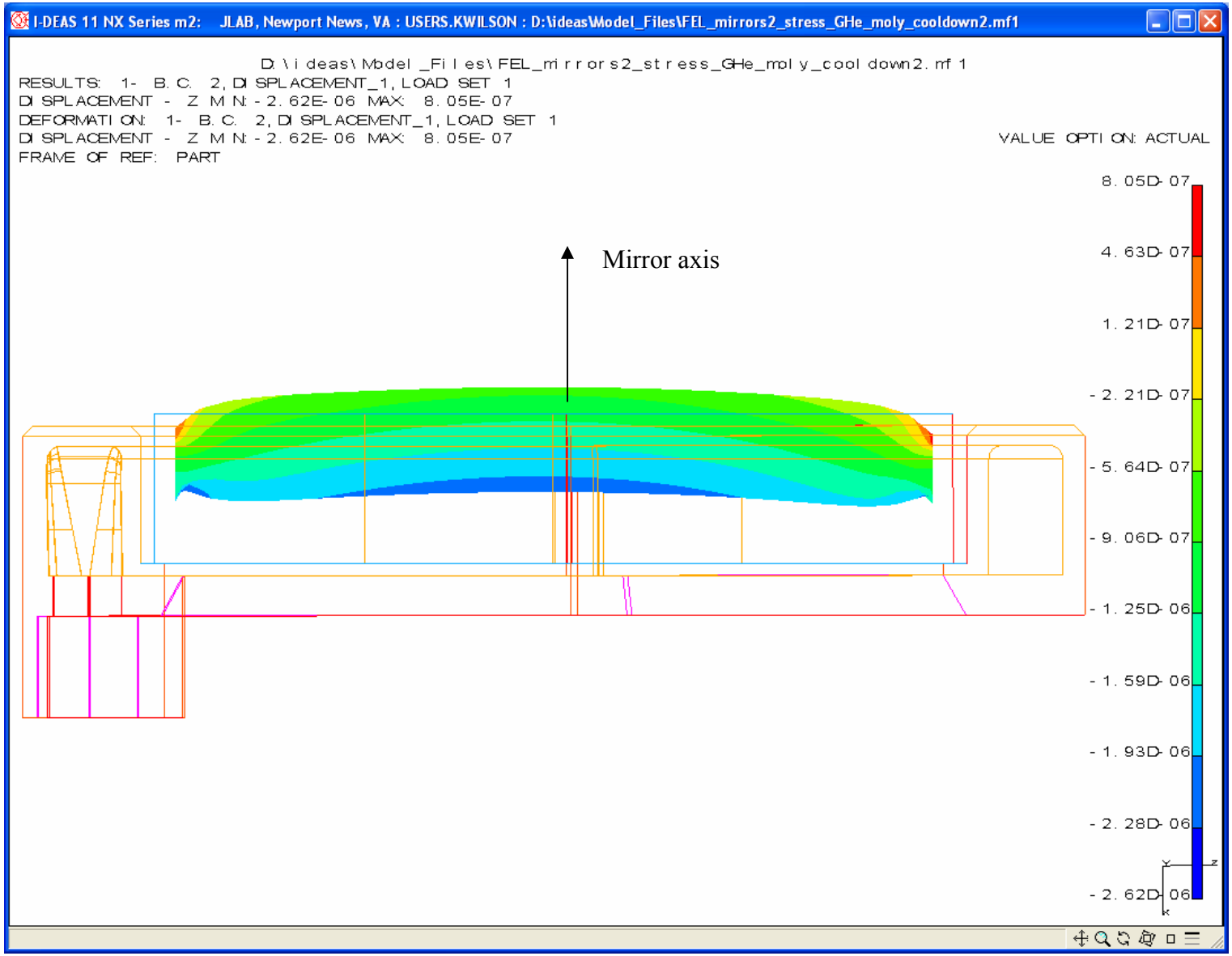


Figure 22: Displacements of cross-section along axis, GHe, molybdenum holder, temperature from 300K to final temperature profile

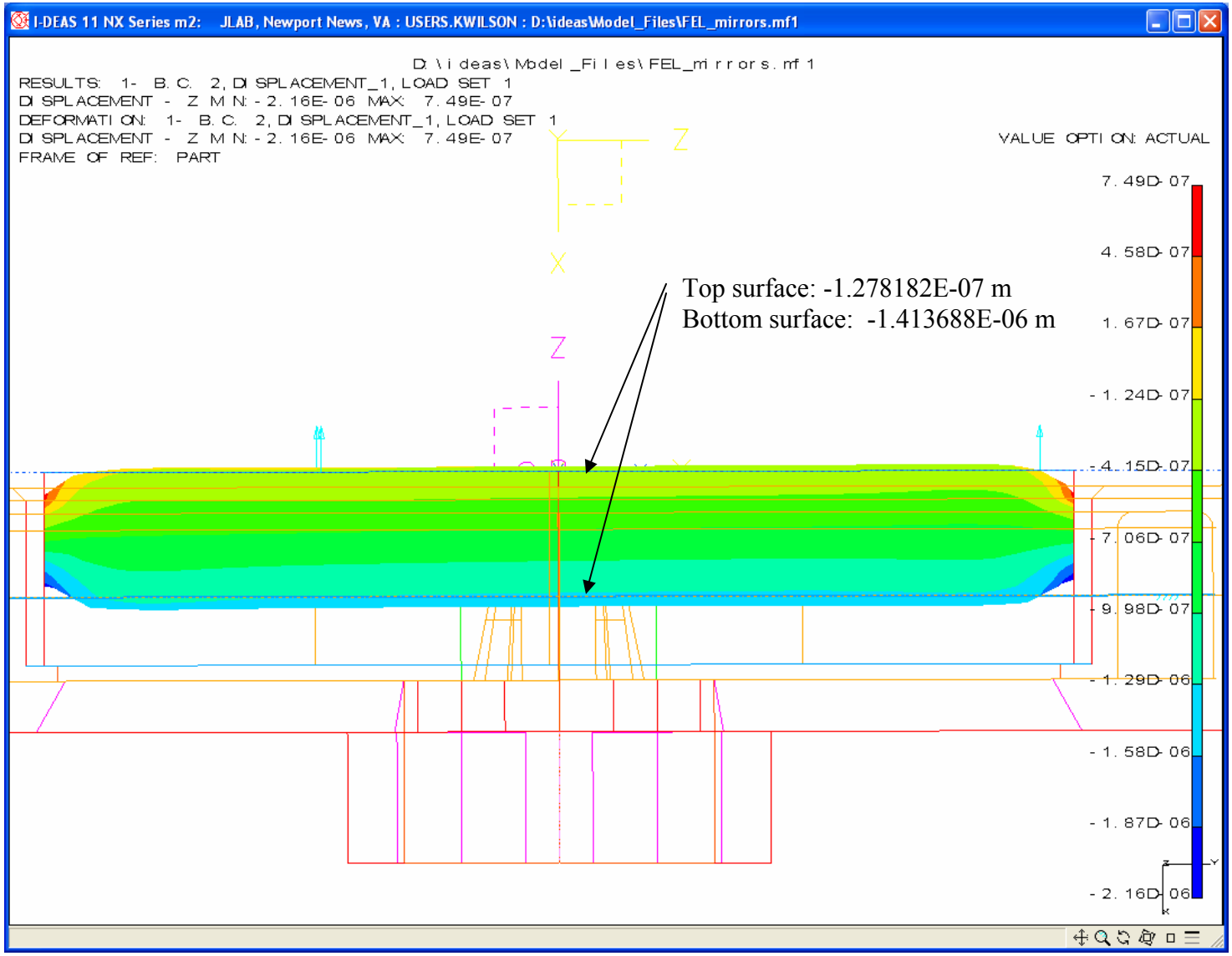


Figure 23: Deformation of mirror alone without holder (temperature from 300K to final temperature profile; temperatures calculated for mirror in molybdenum holder with GHe cooling)

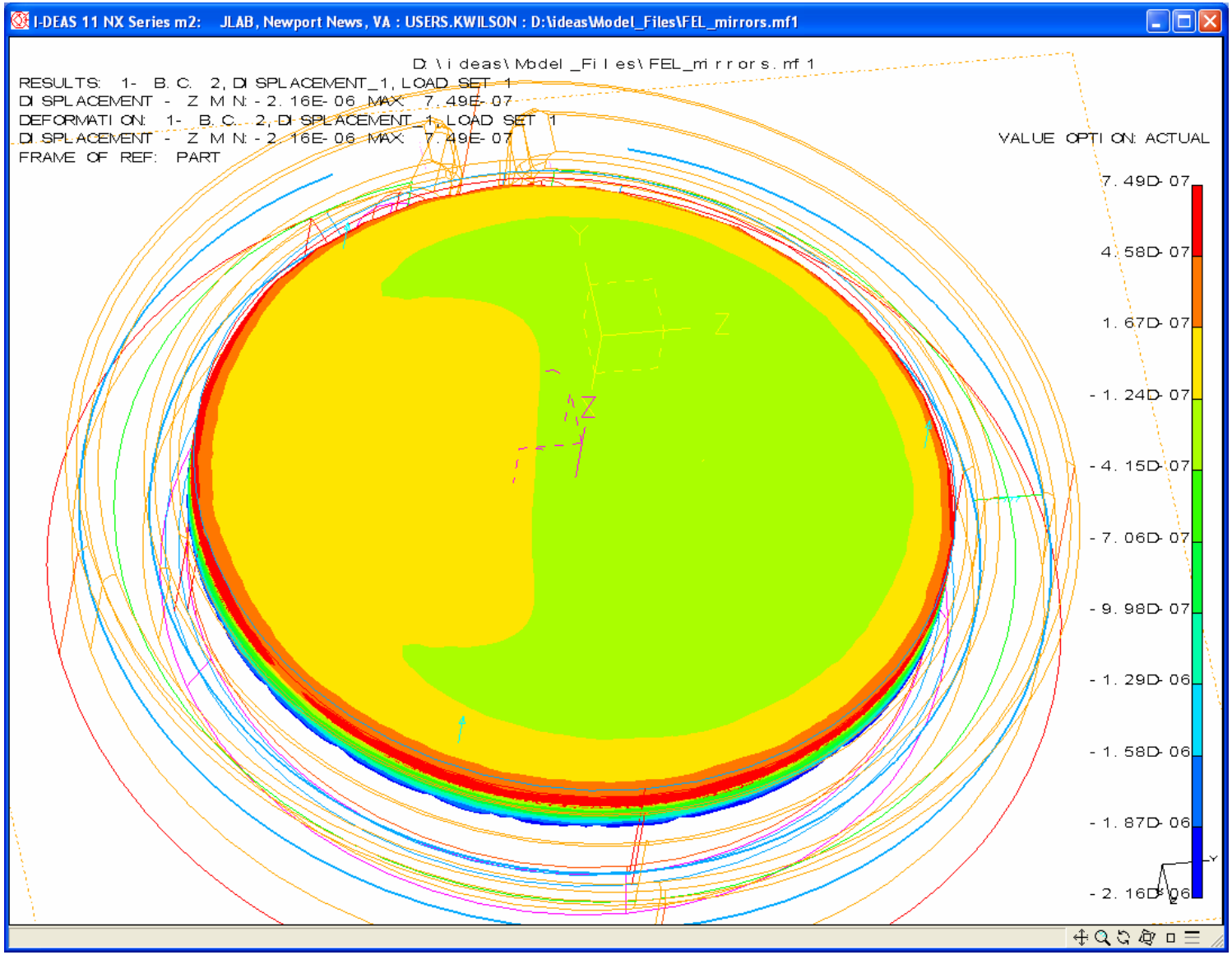


Figure 24: Deformation of mirror alone without holder (temperature from 300K to final temperature profile; temperatures calculated for mirror in molybdenum holder with GHe cooling): top surface

Because the stresses in the indium exceeded its yield, it was necessary to run a plastic analysis to determine the actual stresses and deflections in the mirror. Based on previous analyses, it was clear that a molybdenum holder and gas helium cooling fluid resulted in the lowest stresses, so this was the only model that was evaluated plastically.

Results are shown in the figures below. Although the stresses in the indium change by several orders of magnitude, the changes to the deflections in the indium and mirror are less significant.

For comparison purposes, the plastic models with the stress-strain curve for indium are shown in comparison to the incorrect elastic models that do not include the stress-strain curve.

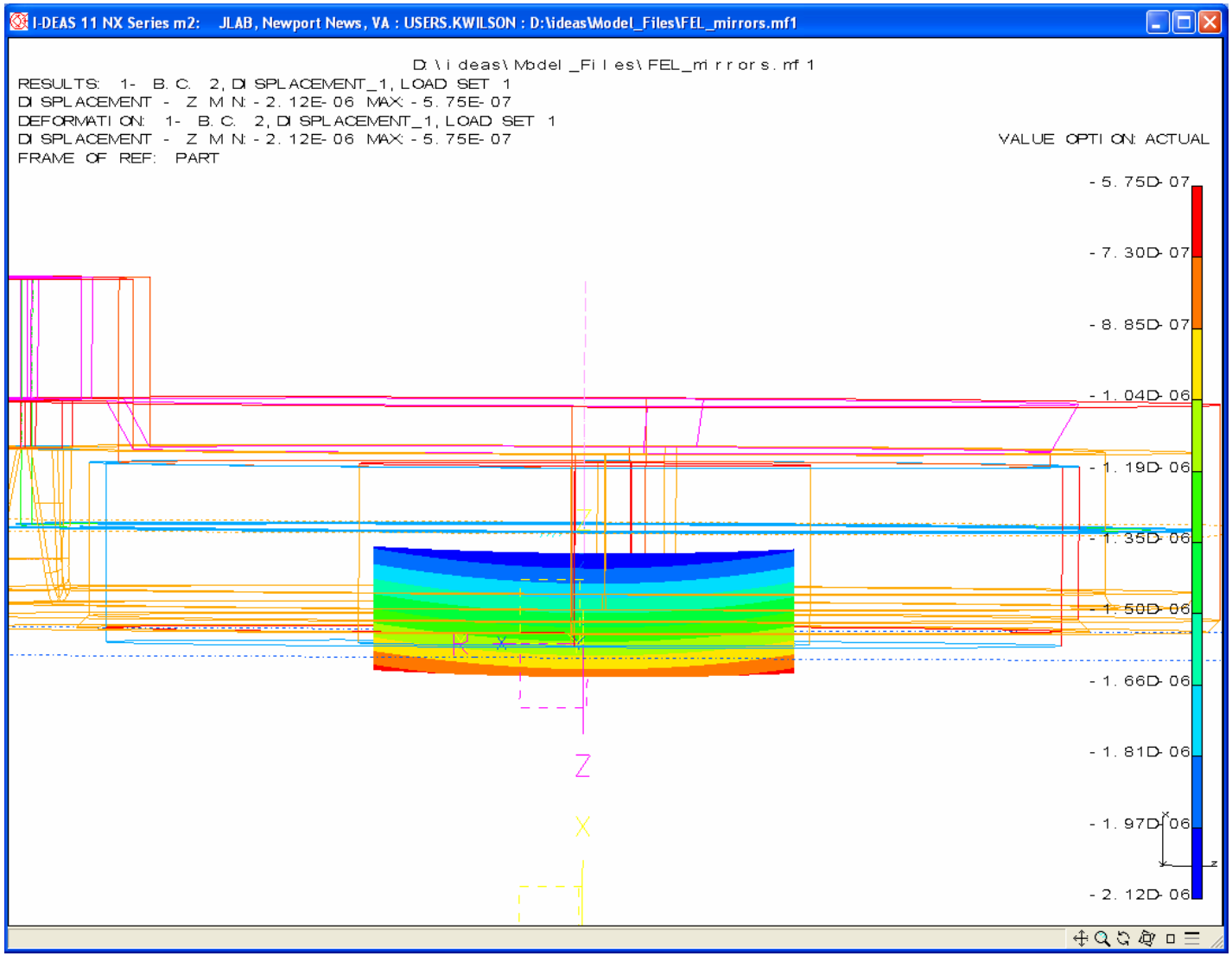

Figure 25: (Incorrect) elastic model: deflections in z of center of mirror; temperature from 300K to final temperature profile

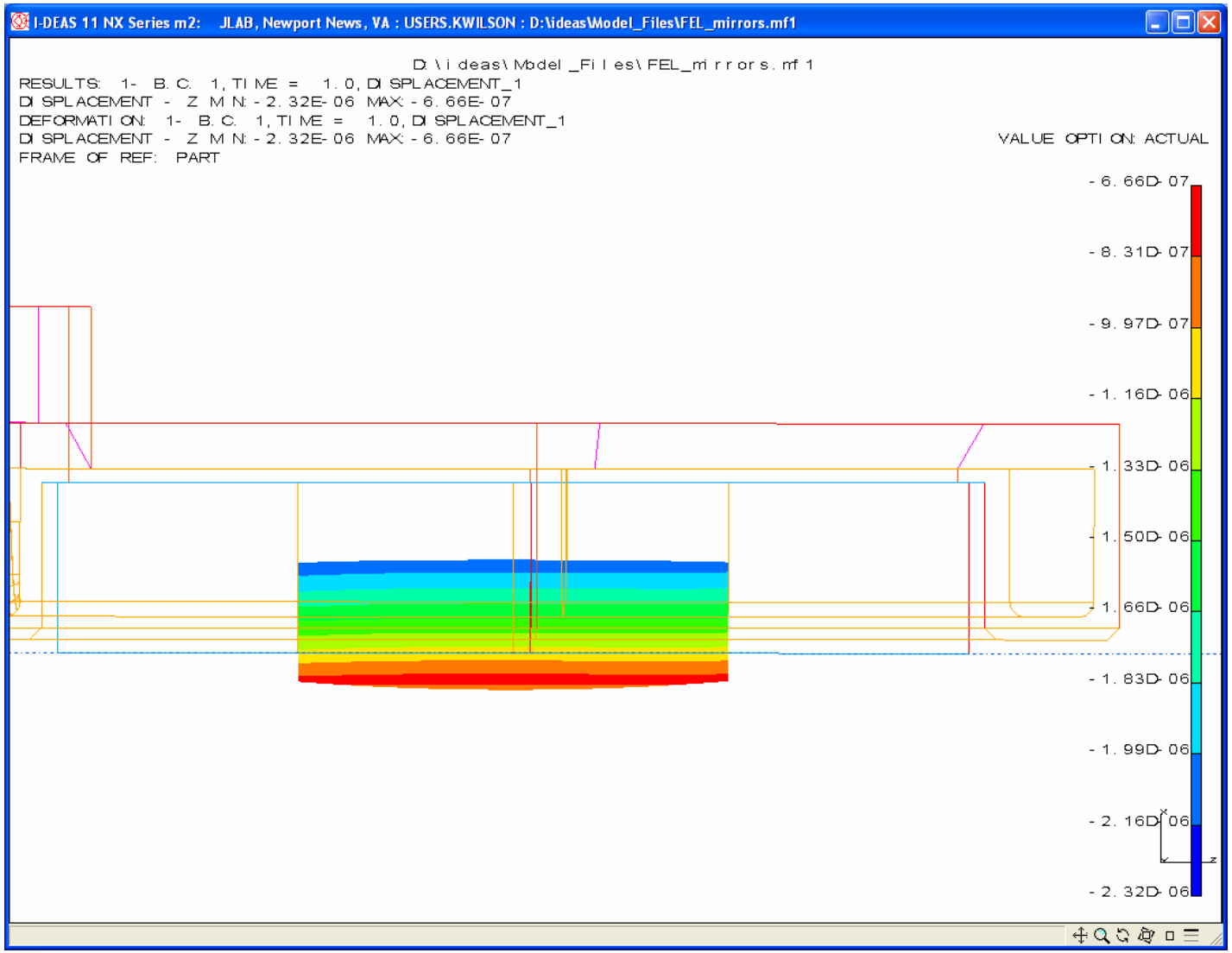

Figure 26: Plastic model: deflections in z of center of mirror; temperature from 300K to final temperature profile

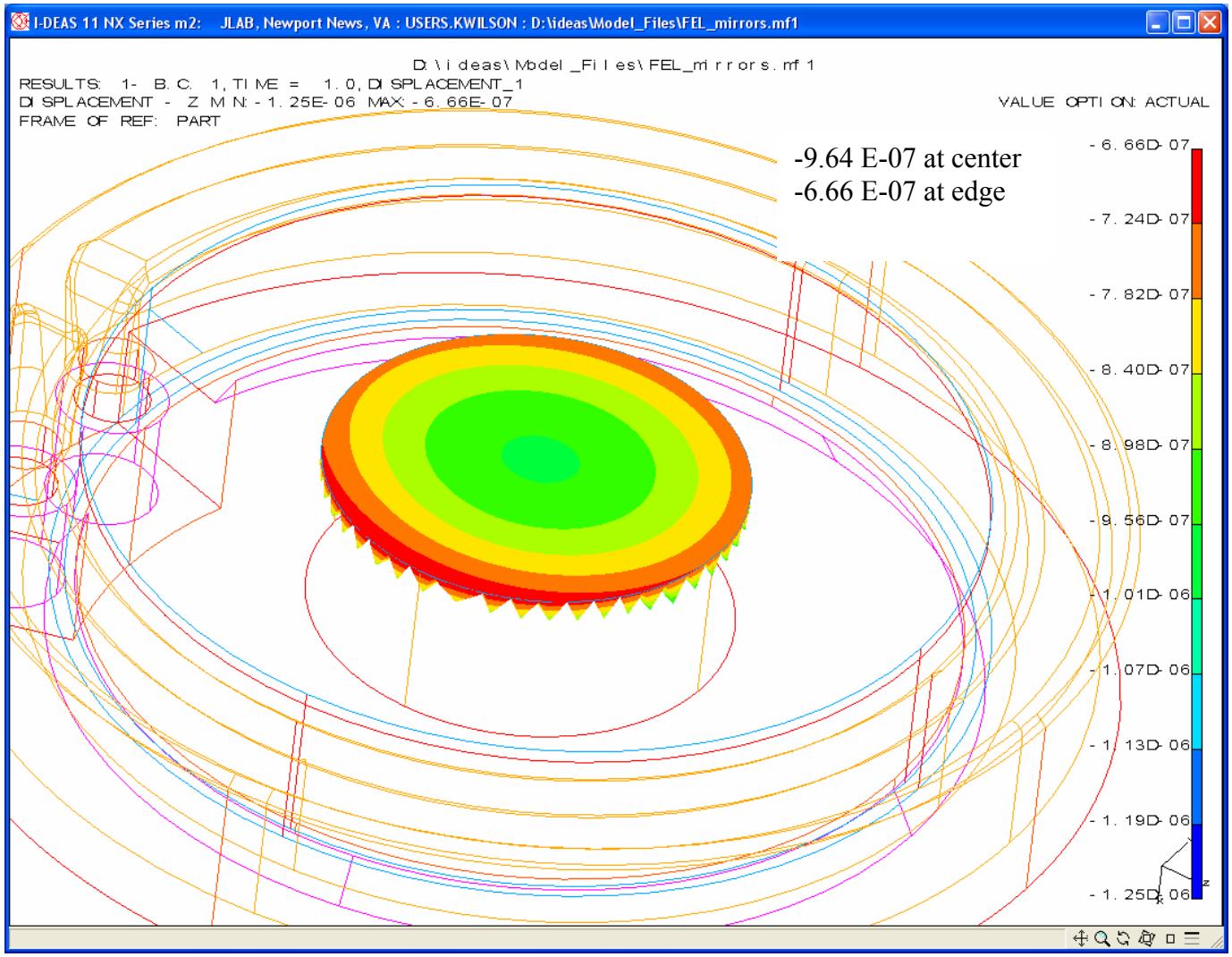

Figure 27: Plastic model: deflections in z of center of top surface of mirror; temperature from 300K to final temperature profile

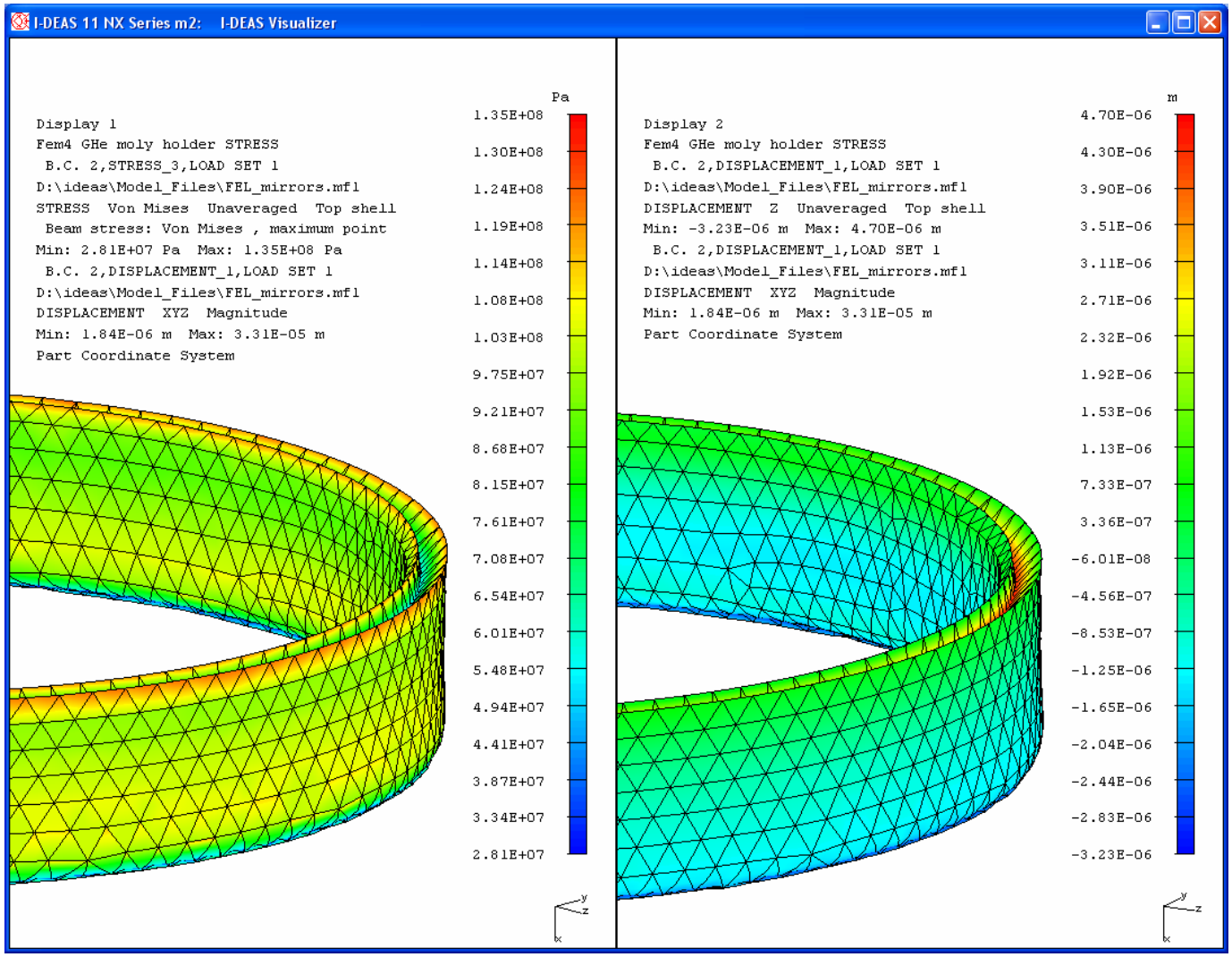


Figure 28: (Incorrect) elastic model: Stresses in indium on the left and displacements in indium in the axial direction on the right; temperature from 300K to final temperature profile

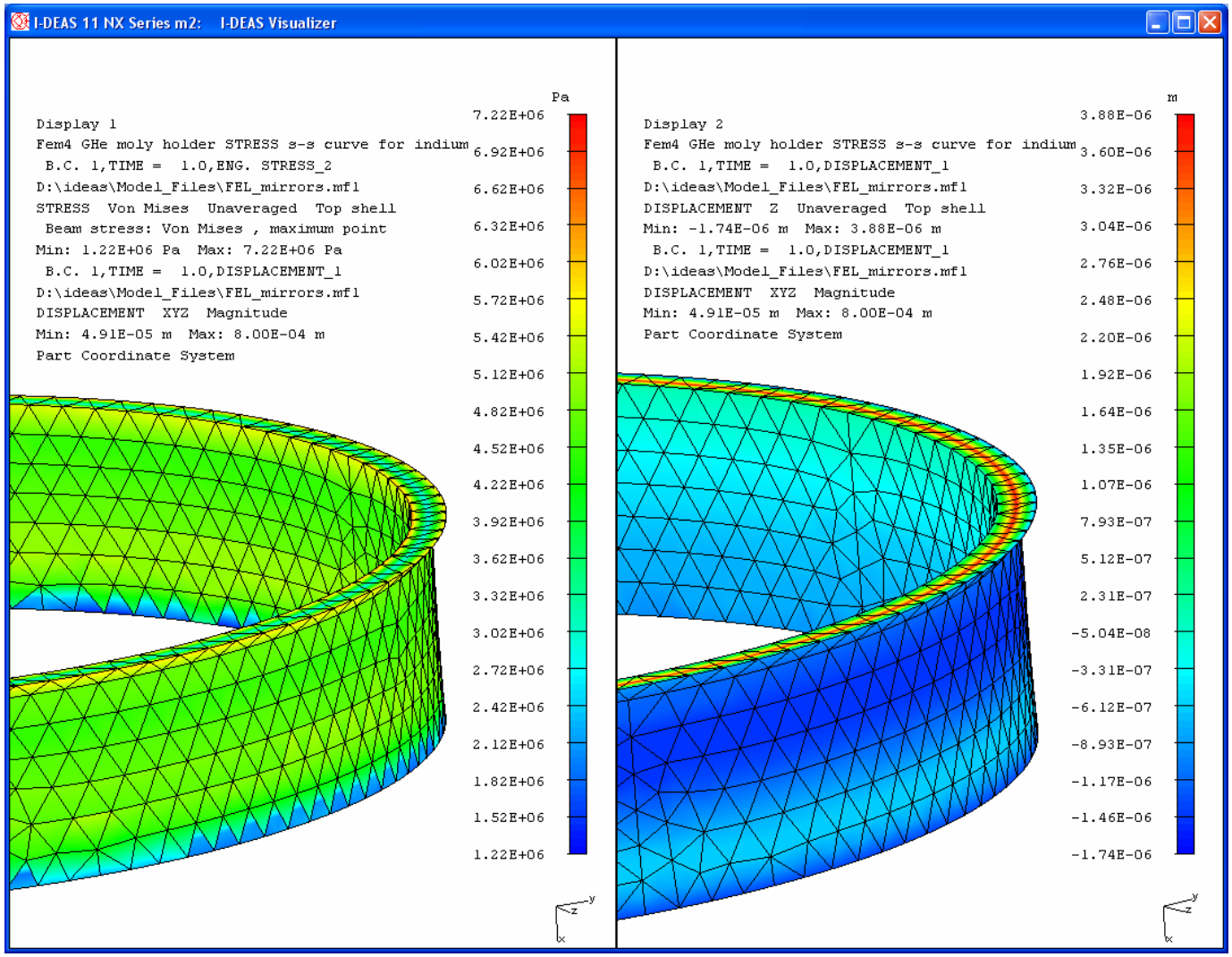


Figure 29: Plastic model: Stresses in indium on the left and displacements in indium in the axial direction on the right; temperature from 300K to final temperature profile

## VI. Conclusions

Even with the optimal materials – a molybdenum holder and gas helium cooling – incorporated into the design, the deflections in the mirror are still significant. While the bulge from the heating alone might fall within the allowable, the mirror also experiences significant bowing or bending from the contraction of the holder during cooldown. This changes the radius of curvature in the mirror from 16 meters to about 16.8 meters.

It should be noted, also, that this analysis only took into account the effects of cooldown from room temperature (300 K) to cryogenic temperatures. In reality, some contractive stresses are generated as well from the cooldown that occurs after brazing when the assembly cools from indium brazing temperature (approximately 430 K) to room temperature.

Further experiments will be done to confirm the analytical results. It is possible that a different design will be required to meet the performance requirements.